

Oxford University Press, Walton Street, Oxford OX2 6DP

Oxford New York
Athens Auckland Bangkok Bombay
Calcutta Cape Town Dar es Salaam Delhi
Florence Hong Kong Istanbul Karachi
Kuala Lumpur Madras Madrid Melbourne
Mexico City Nairobi Paris Singapore
Taipei Tokyo Toronto
and associated companies in
Berlin Brno

Oxford is a trade mark of Oxford University Press

Published in the United States by
Oxford University Press Inc., New York

© J. M. Yeomans 1992

First published 1992

Reprinted 1993, 1994

All rights reserved. No part of this publication may be reproduced, stored in a retrieval system, or transmitted, in any form or by any means, without the prior permission in writing of Oxford University Press. Within the UK, exceptions are allowed in respect of any fair dealing for the purpose of research or private study, or criticism or review, as permitted under the Copyright, Designs and Patents Act, 1988, or in the case of reprographic reproduction in accordance with the terms of licences issued by the Copyright Licensing Agency. Enquiries concerning reproduction outside those terms and in other countries should be sent to the Rights Department, Oxford University Press, at the address above.

This book is sold subject to the condition that it shall not, by way of trade or otherwise, be lent, re-sold, hired out, or otherwise circulated without the publisher's prior consent in any form of binding or cover other than that in which it is published and without a similar condition including this condition being imposed on the subsequent purchaser.

A catalogue record for this book is available from the British Library

Library of Congress Cataloging in Publication Data

Yeomans, J. M.

Statistical mechanics of phase transitions/J. M. Yeomans.

Based on a series of lectures given by the author at Oxford.

Includes bibliographical references.

1. Phase transformations (Statistical physics) I. Title.

QC175.16.P5Y46 1992 530.13—dc20 91-40516

ISBN 0 19 851730 0 (Pbk)

Printed in Great Britain by

Bookcraft (Bath) Ltd, Midsomer Norton, Avon

Preface

The genesis of *Statistical mechanics of phase transitions* lies in a series of lectures I have given to physics graduates and undergraduates at Oxford over the past few years. I hope that it will be of use to future generations of students.

The book is also intended to act as, if not a bridge, a first stepping stone towards an understanding of phase transitions for those beginning research. By providing a summary of the field it may ease the first forays into the research literature.

Many scientists apart from theoretical physicists have an interest in phase transitions. I should be pleased if the book were read by experimentalists and researchers from other disciplines who would like to understand which theoretical approaches are available, when they can be expected to work, and why.

Particular thanks are due to Harvey Dobbs, Dr Philippe Binder, and Professor Eytan Domany for their helpful comments on the manuscript.

Oxford
1991

J.M.Y.

Contents

1	Introduction	1
	1.1 Phase transitions in other systems	4
	1.1.1 A ferrimagnet: cerium antimonide	4
	1.1.2 Surfactants in solution	7
	1.2 A microscopic model	8
	1.2.1 A renormalization group	13
2	Statistical mechanics and thermodynamics	15
	2.1 Statistical mechanics	15
	2.2 Thermodynamics	16
	2.3 Convexity properties of the free energy	19
	2.4 Correlation functions	20
	2.5 First-order and continuous phase transitions	21
	2.6 Critical point exponents	23
	2.6.1 Universality	27
	2.6.2 Exponent inequalities	28
	2.7 Problems	30
3	Models	33
	3.1 The spin-1/2 Ising model	3
	3.1.1 Order-disorder transitions in binary alloys	3
	3.1.2 Lattice gas models	3

3.2	The spin-1 Ising model	41
3.3	The q -state Potts model	41
3.4	X-Y and Heisenberg models	43
3.5	Universality revisited	45
3.6	Discussion	47
3.7	Problems	48
4	Mean-field theories	50
4.1	Mean-field theory for the Ising model	50
4.1.1	Mean-field critical exponents	53
4.2	Landau theory	54
4.2.1	Mean-field critical exponents revisited	56
4.3	The correlation function	57
4.4	Classical mean-field theories	59
4.4.1	Van der Waals theory of fluids	60
4.4.2	Weiss theory of magnetism	61
4.5	The validity of mean-field theory	61
4.6	Problems	63
5	The transfer matrix	67
5.1	Setting up the transfer matrix	67
5.2	The free energy	69
5.3	The correlation function	70
5.4	Results for the Ising model	72
5.4.1	The free energy	73
5.4.2	The magnetization	73
5.4.3	The correlation function	73
5.4.4	The correlation length	74
5.5	Problems	74
6	Series expansions	79
6.1	High temperature series expansions	80
6.2	Low temperature series expansions	85
6.3	The one-dimensional Ising model	86
6.4	Analysis of series expansions	88
6.5	Problems	97
7	Monte Carlo simulations	95
7.1	Importance sampling	99
7.2	Practical details	97
7.3	Considerations in the data analysis	100
7.3.1	Influence of the starting configuration	100
7.3.2	Statistical errors	100
7.3.3	Finite-size corrections	100
7.4	Examples	100
7.4.1	The three-dimensional Ising model	100
7.4.2	More complicated systems	100
7.5	Problem	100
8	The renormalization group	100
8.1	Definition of a renormalization group transformation	100
8.2	Flows in parameter space	100
8.3	Universality	111
8.3.1	Crossover	111
8.4	An example	111
8.5	Scaling and critical exponents	111
8.6	Scaled variables	111
8.7	Conformal invariance	111
8.8	Problems	111
9	Contents	ix

9 Implementations of the renormalization group 124

9.1	The one-dimensional Ising model	124
9.1.1	Derivation of the recursion equations	125
9.1.2	Fixed points	127
9.1.3	Fixed points and scaling	129
9.1.4	The free energy	130
9.2	Higher dimensions	132
9.3	The q -state Potts model	136
9.4	The Monte Carlo renormalization group	139
9.5	The ϵ -expansion	140
9.6	Problems	141

Further reading 145

Index 147

1

Introduction

A phase transition occurs when there is a singularity in the free energy or one of its derivatives. What is often visible is a sharp change in the properties of a substance. The transitions from liquid to gas from a normal conductor to a superconductor, or from paramagnet to ferromagnet are common examples.

The phase diagram of a typical fluid is shown in Fig. 1.1. As the temperature and pressure are varied water can exist as a solid, a liquid or a gas. Well-defined phase boundaries separate the regions in which each state is stable. Crossing the phase boundaries there is a jump in the density and a latent heat, signatures of a first-order transition.

Consider moving along the line of liquid-gas coexistence. As the temperature increases the difference in density between the liquid and the gas decreases continuously to zero as shown in Fig. 1.2. It becomes zero at the critical point beyond which it is possible to move continuously from a liquid-like to a gas-like fluid. The difference in densities which becomes non-zero below the critical temperature, is called the order parameter of the liquid-gas transition.

Seen on the phase diagram of water the critical point looks insignificant. However, there are clues that this might not be the case. Fig. 1.3 shows the specific heat of argon measured along the critical isochore $\rho = \rho_c$. There is a striking signature of criticality: the specific heat diverges and is infinite at the critical temperature itself.

Analogous behaviour is seen in magnetic phase transitions. The phase diagram of a simple ferromagnet is shown in Fig. 1.4. Just as in the case of liquid-gas coexistence there is a line of first-order transition ending in a critical point. All transitions occur at zero magnetic field $H = 0$, because of the symmetry of a ferromagnet to reversals in the field. The additional symmetry means that it is often easier to work in magnetic language and we shall do so throughout most of this book.

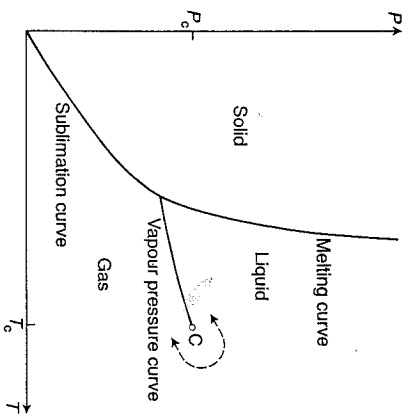


Fig. 1.1. Phase diagram of a fluid. All the phase transitions are first-order except at the critical point C . Beyond C it is possible to move continuously from a liquid to a gas. The boundary between the solid and liquid phases is thought to be always first-order and not to terminate in a critical point.

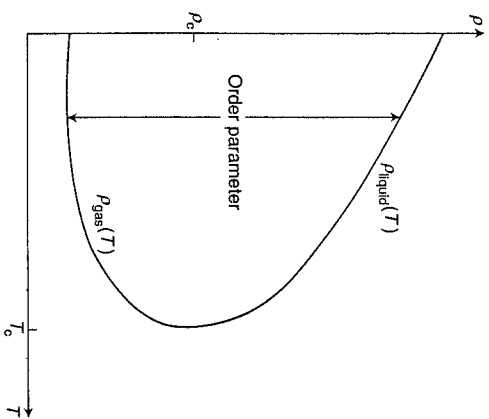


Fig. 1.2. Values of the densities of the coexisting liquid and gas along the vapour pressure curve. $(\rho_{\text{liquid}}(T) - \rho_{\text{gas}}(T))$ is the order parameter for the liquid-gas transition.

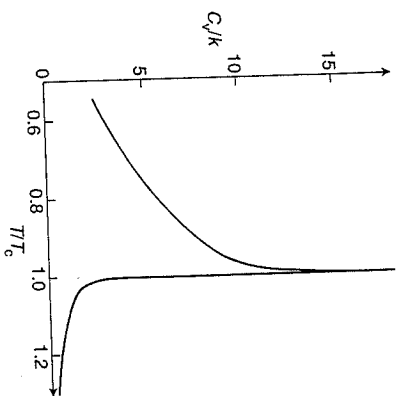


Fig. 1.3. Specific heat at constant volume of argon measured on the critical isochore, $\rho = \rho_c$. After Fisher, M.E. (1964). *Physical Review*, 136A, 1599.

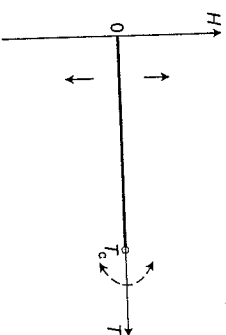


Fig. 1.4. Phase diagram of a simple ferromagnet. A line of first-order transitions at zero field ends in a critical point at a temperature T_c .

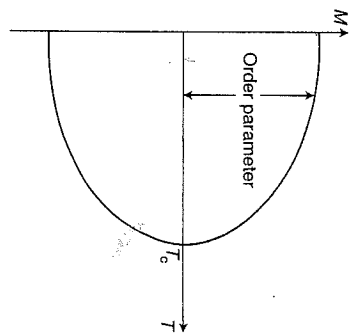


Fig. 1.5. Zero-field magnetization of a ferromagnet. Below the critical temperature there is a spontaneous magnetization $\pm M(T)$.

Crossing the phase boundary at temperatures less than the critical temperature, there is a jump in the magnetization. Above the critical temperature it is possible to move continuously from a state of negative magnetization to one of positive magnetization. The critical point itself separates these two behaviours; the magnetization is continuous but its derivatives are discontinuous. This manifests itself, just as in the fluid case, by divergences in the response functions, the specific heat and the susceptibility.

The order parameter for the ferromagnetic phase transition is the magnetization. Its variation with temperature along the coexistence curve, $H = 0$, is shown in Fig. 1.5. Compare this diagram with Fig. 1.2 for the fluid; the only difference is the extra symmetry in the magnetic case.

1.1 Phase transitions in other systems

Phase transitions in fluids and ferromagnets provide two simple examples of an enormous diversity of changes of state. Table 1.1 lists other examples, together with references for those wishing to pursue them further. We describe two cases in more detail to illustrate the richness and complexity of the phase diagrams found in nature.

1.1.1 A ferrimagnet: cerium antimonide

In cerium antimonide, strong uniaxial spin anisotropy constrains the spins to lie along the [100] direction. Within the (100) planes the

Table 1.1. Examples of the diversity of phase transitions found in nature

Transition	Example	Order parameter
ferromagnetic ^a	Fe	magnetization
antiferromagnetic ^a	MnO	sublattice magnetization
ferrimagnetic ^a	Fe ₃ O ₄	sublattice magnetization
structural ^b	SrTiO ₃	atomic displacements
ferroelectric ^b	BaTiO ₃	electric polarization
order-disorder ^c	CuZn	sublattice atomic concentration
phase separation ^d	CCl ₄ +C ₇ F ₁₆	concentration difference
superfluid ^e	liquid ⁴ He	condensate wavefunction
superconducting ^f	Al, Nb ₃ Sn	ground state wavefunction
liquid crystalline ^g	rod molecules	various

^aKittel, C. (1976). *Introduction to solid state physics* (6th edn). (Wiley, New York).

^bBruce, A. D. and Cowley, R. A. (1981). *Structural phase transitions*. (Taylor and Francis, London).

^cAls-Nielsen, J. (1976). Neutron scattering and spatial correlation near the critical point. In *Phase transitions and critical phenomena*, Vol. 5a (eds C. Domb and M. S. Green), p. 87. (Academic Press, London).

^dRowlinson, J. S. and Swinton, F. L. (1982). *Liquids and liquid mixtures* (3rd edn). (Butterworth Scientific, London).

^eWilks, J. and Betts, D. S. (1987). *An introduction to liquid helium* (2nd edn). (Clarendon Press, Oxford).

^fM^cClintock, P. V. E., Meredith, D. J., and Wignmore, J. K. (1984). *Matter at low temperatures*. (Blackie, Glasgow and London).

^gde Gennes, P.-G. (1974). *The physics of liquid crystals*. (Oxford University Press, Oxford).

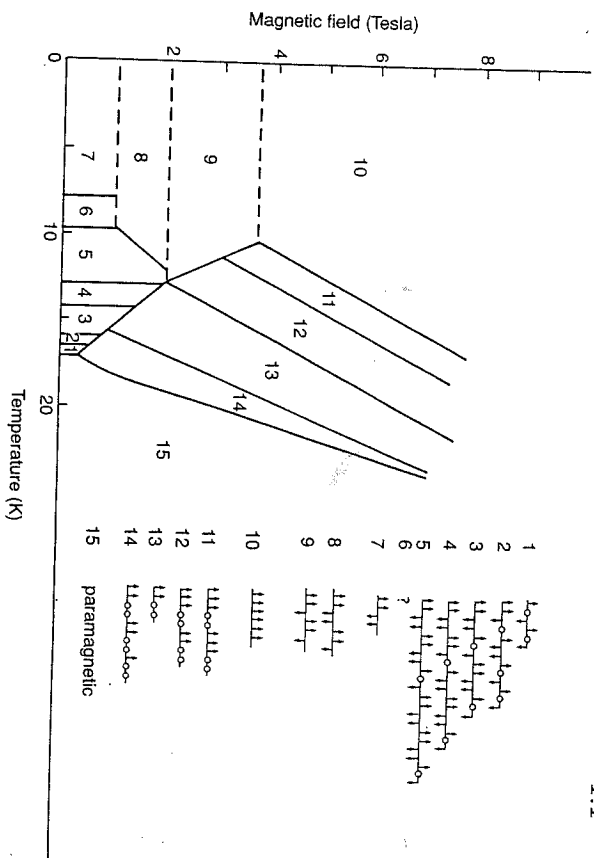


Fig. 1.6. The ferromagnetic phases of cerium antimonide. The relative ordering of successive ferromagnetic planes in each phase is indicated in the Figure. \circ denotes a plane with a net magnetization of zero. After Rossat-Mignod, J., Burlet, P., Bartholin, H., Vogt, O., and Lagnier, R. (1980). *Journal of Physics C: Solid State Physics*, **13**, 6381, Institute of Physics Publishing Limited.

ordering is ferromagnetic: most planes lie in a state with spins $s = +1$ or $s = -1$, although planes with a net magnetization of zero are also observed. The relative ordering of the planes themselves is ferrimagnetic. Fourteen different states, separated by first-order phase boundaries, have been identified in neutron scattering experiments. These differ in the relative alignment of successive planes and are identified in the phase diagram shown in Fig. 1.6. Note the patterns that link the various sequences of phases: similar patterns are seen in series of first-order transitions in binary alloys and minerals¹.

¹Yeomans, J.M. (1988). The theory and application of axial Ising models. In *Solid state physics*, Vol. 41 (eds H. Ehrenreich, F. Seitz, and D. Turnbull), p.151. (Academic Press, New York).

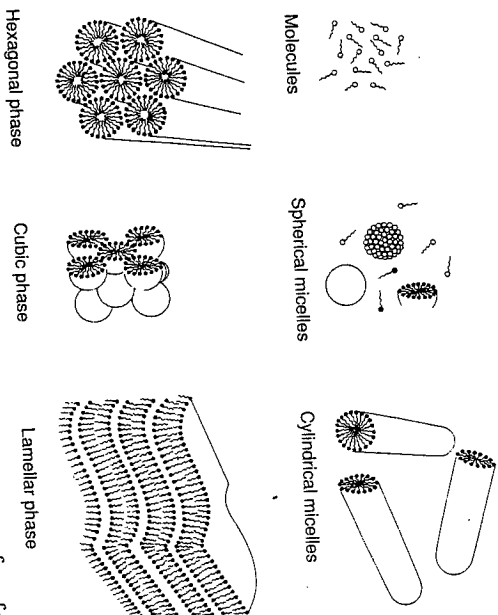


Fig. 1.7. Schematic drawings of the idealised structures of surfactant molecules that can form in solution as the surfactant concentration is increased. After Corkhill, J. M. and Goodman, J. F. (1969). *Advances in Colloid and Interface Science*, **2**, 297.

1.1.2 Surfactants in solution

Solutions of surfactant molecules have exotic phase diagrams². These molecules have a polar head group which is very soluble in water and hydrocarbon tail which is only just soluble. Hence they like to position themselves in such a way that the head is next to water molecules and the tail is shielded from them. If there is a surface they will migrate there and sit head-down. This lowers the surface tension—hence the use as soaps.

The phase diagrams of solutions of surfactant molecules are determined mainly by the concentration of the solute. As this increases micelles form. These are groups of molecules arranged in a sphere cylinder so that the polar heads shield the hydrocarbon tails from the water. A further increase in concentration can lead to a phase transition to a state consisting of micelles ordered in a hexagonal or cubic array with the intervening spaces filled with water. A second transition is also observed in some systems. This is to a lamellar phase where the molecules are arranged into sheets but move freely within the sheet

²The future of industrial fluid design. In *Chemistry in Britain*, **28**, 4, April (1990).

like a two-dimensional liquid. Fig. 1.7 illustrates some of the possible phases.

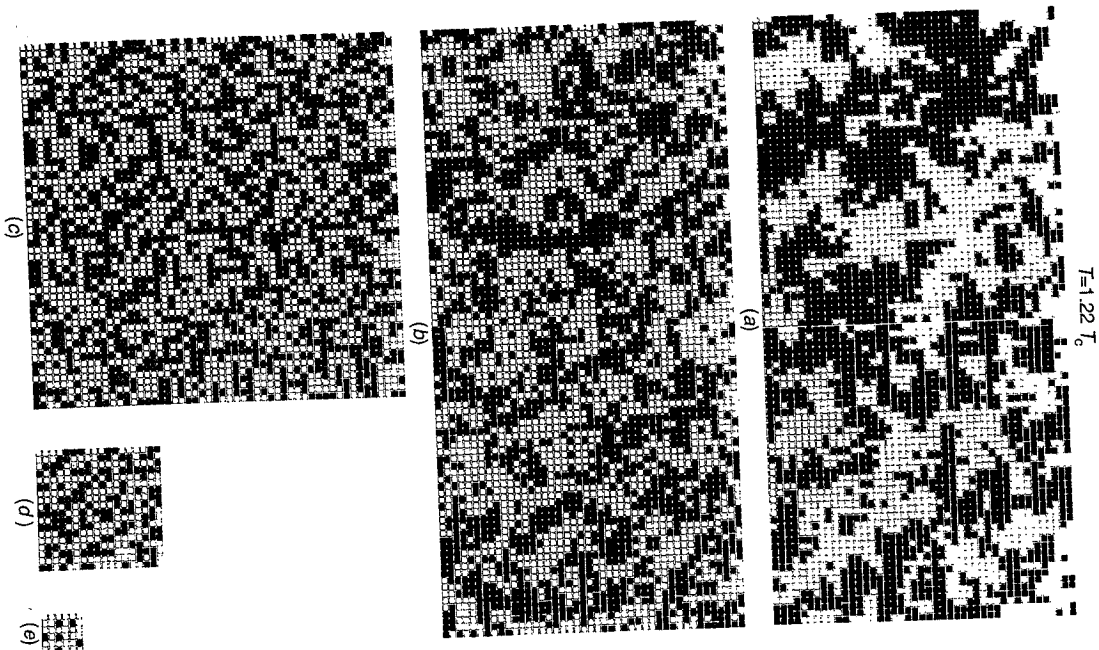
Fluids, magnets, superconductors, surfactants: all apparently very different systems. Can the phase transitions associated with such diverse types of order be brought within the same theoretical framework? Why is there an order parameter, such as the magnetization, which becomes non-zero within the ordered phase? Why and how do the response functions diverge at the critical temperature? The aim of this book is to give an introduction to the theories that have been developed to answer these questions. A first step is to describe what is happening on a microscopic level at a phase transition with the aim of understanding the physics underlying the properties of a system at criticality.

1.2 A microscopic model

Consider a simple model of a two-dimensional interacting system, the Ising model on a square lattice. On each lattice site i there is a variable, called for convenience a spin, which can take two different values, $s_i = +1$ or $s_i = -1$. Each spin interacts with its nearest neighbours on the lattice through an exchange interaction, J , which favours parallel alignment

$$\mathcal{H} = -J \sum_{\langle ij \rangle} s_i s_j \quad (1.1)$$

Fig. 1.8. A real-space renormalization group transformation for the two-dimensional Ising model on the square lattice. The initial configuration, corresponding to a temperature $T = 1.22T_c$, was generated using a Monte Carlo simulation. A sequence of renormalized configurations is then obtained by replacing successive clusters of nine spins by a single spin which takes the same value as the majority of the spins in the original cluster. Hence the length scale of the lattice is changed by a scale factor $b = 3, 3^2, 3^3$, and 3^4 in (b), (c), (d), and (e) respectively. Note that the correlation length decreases under successive iterations of the renormalization group corresponding to an increase in the temperature. After Wilson, K. G. (1979). *Scientific American*, 241, 140.



where we use the notation $\langle ij \rangle$ to represent a sum over nearest neighbour spins on sites i and j .

The two-dimensional Ising model has been solved exactly and is known to have a phase diagram like that shown in Fig. 1.4 with a continuous phase transition at zero field and a temperature T_c . The magnetization becomes non-zero at the critical temperature and increases to its saturation value, which corresponds to all the spins being aligned, at $T = 0$, just as in Fig. 1.5.

To see what is happening to individual spins as the temperature is changed it is not difficult to simulate the model on a computer with the fluctuations characteristic of finite temperatures being mimicked by a random number generator. This is the Monte Carlo method which will be described in more detail in Chapter 7. The results are shown in Figs 1.8–1.10. Black squares are used to represent spin $s_i = +1$ and white squares $s_i = -1$.

At temperatures very much greater than the critical temperature entropic contributions dominate the exchange energy and, although nearest neighbours tend to lie parallel, this is a small perturbation on a random configuration. Fig. 1.8(c) is an example of this. As the temperature is lowered the effects of the exchange interaction become more apparent. Nearest neighbours become more likely to point in the same direction and clusters of aligned or correlated spins appear. The size of the largest clusters is measured by a length called the correlation length. In Fig. 1.8(a) where the temperature is $1.2T_c$ the correlation length is of the order of a few lattice spacings. The system is said to show short-range order.

As the temperature is lowered the correlation length increases. Note, however, that fluctuations on a smaller scale remain important; there are correlated regions of spins on *all* length scales up to that set by the correlation length. Each fluctuation is not an area of uniform spin alignment but includes smaller fluctuations which in turn include yet smaller ones down to the length scale set by the lattice spacing...

Clusters contain lesser ones

Complicating quite 'em

And lesser ones have lesser still

Inside, *ad infinitum*.

(adapted from Jonathan Swift)

The critical temperature itself is marked by the correlation length becoming infinite. A typical spin configuration at the critical temperature is shown in Fig. 1.9(a). There is now no upper length cut-off and ordered structures exist on every length scale. This is the microscopic

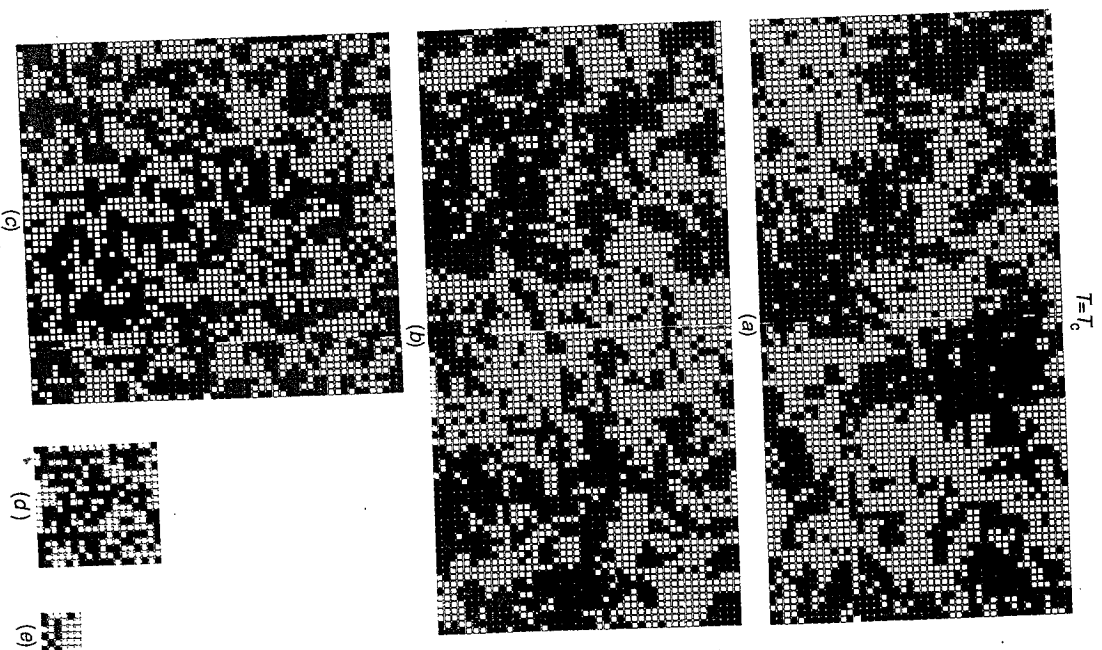


Fig. 1.9. As Fig. 1.8 but with a starting temperature $T = T_c$. Because the correlation length is initially infinite there is no change in the ordered state under iteration of the renormalization group and the system remains at the critical temperature. After Wilson, K. G. (1979). *Scientific American*, 241, 140.

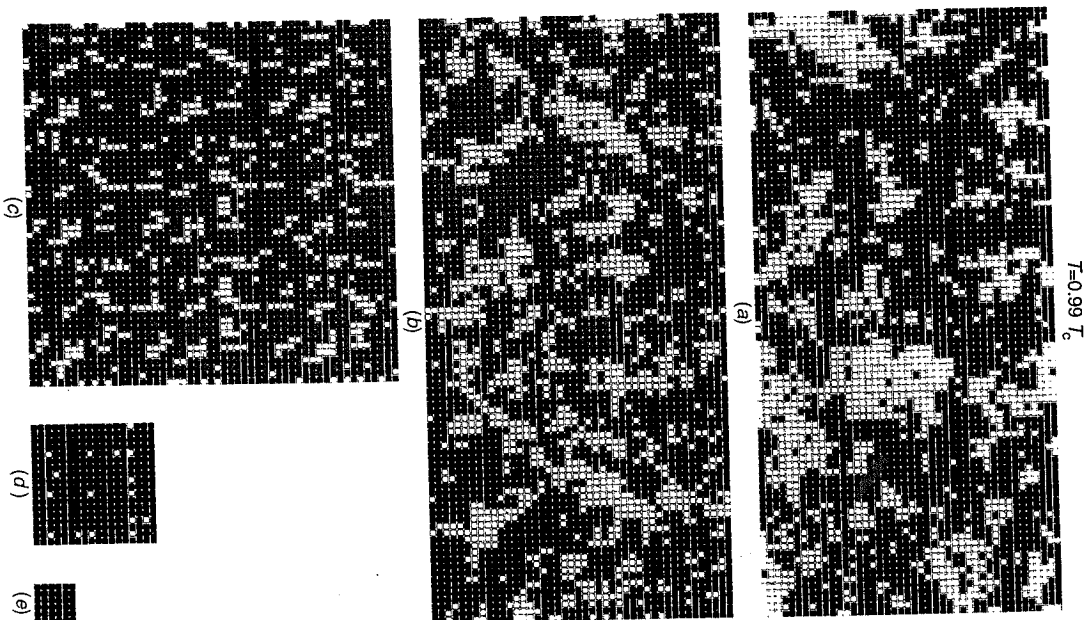


Fig. 1.10. As Fig. 1.8 but with a starting temperature $T = 0.99T_c$. Fluctuations relative to the ordered state are suppressed by the change in length scale and the system flows towards zero temperature. After Wilson, K. G. (1979). *Scientific American*, 241, 140.

physics which underlies a critical phase transition. *Fluctuations on all scales of length are important.*

Below the critical temperature there is a non-zero magnetization. More spins lie in one of the two spin states: in Fig. 1.10 this is spin-up or black. The model is said to exhibit long-range order. At zero temperature all the spins are aligned because of the exchange interaction. As the temperature increases entropic terms in the free energy lead to fluctuations away from this state and the magnetization drops from its saturated value. Fig. 1.10(c) shows a spin configuration for a temperature $T \ll T_c$. The correlation length measures the size of the largest fluctuations away from the ordered background. As the temperature increases towards the critical temperature the correlation length becomes larger. Just as for $T > T_c$, there are clusters embedded within clusters on all length scales. The fluctuations cause the magnetization to fall, and it drops to zero exactly at the critical temperature where the correlation length becomes infinite and the underlying order is completely destroyed.

The long-range fluctuations in the magnetization of magnetic systems near the critical point are mirrored by long-range fluctuations in the density of fluid systems. These can be observed directly. If light is shone on to a fluid near its critical temperature it is reflected strongly, causing the fluid to appear milky-white. The strong scattering appears when the density fluctuations become of a size comparable to the wavelength of light, about a thousand times the interatomic spacing. This critical opalescence persists throughout the critical region emphasizing that fluctuations at this length scale remain important even though the maximum length scale increases to infinity (mm or cm in a real sample).

1.2.1 A renormalization group

We have stressed that, at a critical point, all length scales are important. This is an unusual situation: usually physical theories can concentrate on a small range of scales of length. A continuum theory of water waves, ignoring atomic motions, or a theory of the arrangement of nucleons which ignores the atomic environment are essentially exact. So how can we cope with, or even exploit, scale invariance at criticality?

The answer lies in a set of theories known as renormalization groups. These will be described in much more detail in Chapters 8 and 9 but the ideas behind them can be illustrated using the Monte Carlo simulations in Figs 1.8–1.10. The aim is to change the scale of the system and see how it behaves. This is done by taking each group of nine spins in turn

and replacing it by a single spin which takes the same value as the majority of spins in the original cluster. This procedure reduces the scale of the system by a factor $b = 3$. We then keep going to produce the series of snapshots of the spin configuration, essentially seen under different magnifications, shown in the figures.

For a starting temperature above the critical temperature (Fig. 1.8), the scale change soon obliterates any short-range order and the spins on the renormalized lattices become uncorrelated. This corresponds to an infinite temperature: the system has been renormalized by the simple transformation we have defined to $T = \infty$. This will be the case for all temperatures above T_c ; the nearer to the critical temperature is the starting point the more steps of the transformation it will take to lose the short-range order.

For temperatures below the critical temperature there is an analogous flow as the renormalization group is iterated. However, now any fluctuations are relative to the ground state and, as these are lost under renormalization, the system flows to a completely ordered state characteristic of zero temperature. This is the case in Fig. 1.10.

Only at the critical temperature itself, Fig. 1.9, where there are fluctuations on all length scales does the system remain invariant under the renormalization group transformation. This can be exploited to identify the critical point and describe the behaviour of the thermodynamic functions in its vicinity.

2

Statistical mechanics and thermodynamics

This chapter moves through the large number of reminders and details necessary to arrive at the point where we can introduce the idea of universality, one of the most striking features of the theory of critical phenomena and a major justification for the interest in models. The first step is to summarize the statistical mechanics used throughout the book. Assuming that this is familiar material the main aim will be to gather together the relevant formulae in a form suitable for reference.

We then describe in more detail the behaviour of the thermodynamic functions at a phase transition, distinguishing between first order and continuous transitions. It is very important to find a way of describing the asymptotic behaviour of these functions near a continuous transition and, to this end, we introduce the critical point exponents. A discussion of why they play a central role in the theory leads to the concept of universality.

2.1 Statistical mechanics

We assume that the reader is sufficiently familiar with elementary statistical mechanics to regard it as reasonable to start from the canonical partition function

$$Z(T, H) = \sum_r e^{-\beta E_r} \quad (2)$$

where the sum is over all states r with energy E_r and $\beta = 1/kT$ with Boltzmann's constant and T the temperature. Most of the subsequent chapters of this book will be concerned with models which, even if not applied to magnetic systems, are written in magnetic language, and therefore it is convenient to consider an ensemble in which Z depends

on the temperature and the field H . Maxwell-Boltzmann statistics are appropriate because the magnetic systems we consider will consist of localized, and hence distinguishable, spins and the fluid systems will be in the classical regime.

The free energy is proportional to the logarithm of the partition function

$$\mathcal{F}(T, H) = -kT \ln Z(T, H). \quad (2.2)$$

All macroscopic thermodynamic properties follow from differentiating the free energy. The relevant formulae are listed in Tables 2.1 and 2.2 for magnetic and fluid systems respectively. Readers unfamiliar with these should consult a text on statistical mechanics such as Callen¹. Those who are rusty might find it helpful to try problems 2.1 and 2.2.

Often our aim will be to calculate the free energy. However, sometimes, particularly in numerical work, it is easier to extract properties such as the magnetization or the energy directly.

2.2 Thermodynamics

For a magnetic system the first law of thermodynamics can either be written²

$$dU = T dS - M dH \quad (2.3)$$

or

$$d\tilde{U} = T dS + H dM \quad (2.4)$$

where dU , dS , dH , and dM are the changes in the energy, entropy, magnetic field, and magnetization respectively. We have assumed the volume V is fixed and hence omitted the term $-PdV$. Both forms of the first law are equally valid but they correspond to different definitions of the energy. The energy stored in the applied magnetic field is not included in U , whereas it is included in \tilde{U} .

We shall use eqn (2.3) throughout because the free energy will then depend on the most convenient variables (T, H) and will be identical

¹Callen, H. B. (1985). *Thermodynamics and an introduction to thermostatistics* (2nd edn). (Wiley, New York).

²The 'field' H , is taken to have the units of energy and the 'magnetization', M , to be dimensionless as is customary when writing spin Hamiltonians. If the field is the result of a magnetic field, B , they are related by $H \sim \mu_B B$ where μ_B is the Bohr magneton.

Table 2.1. The relation of the thermodynamic variables pertinent to a magnetic system to the partition function

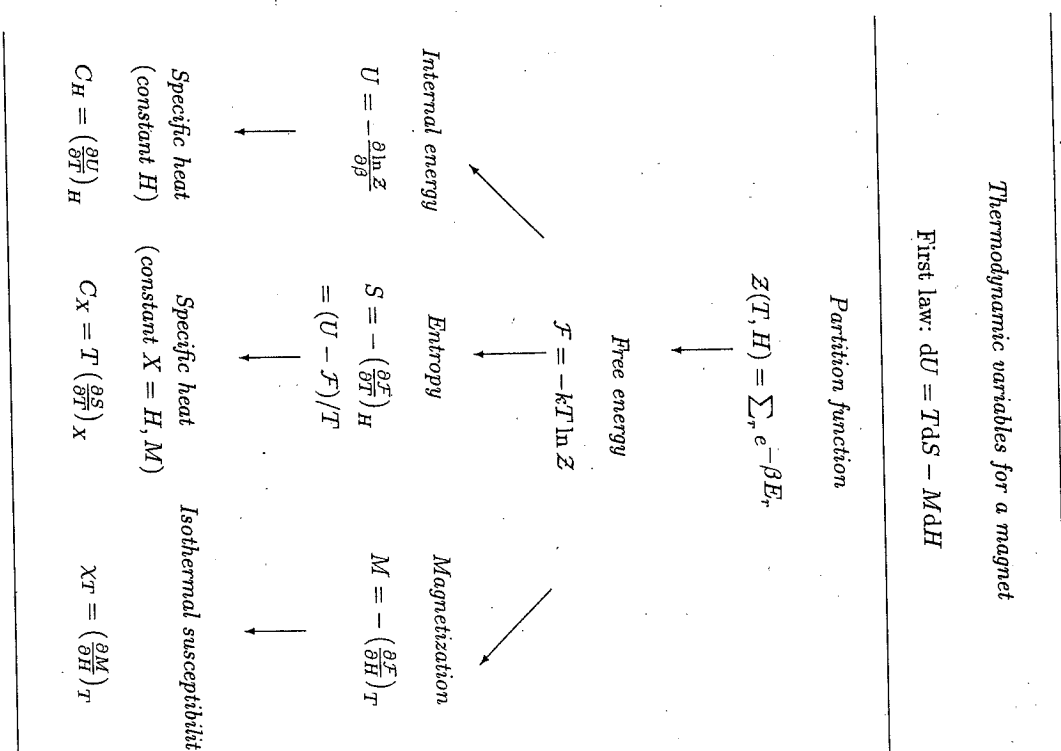


Table 2.2. The relation of the thermodynamic variables pertinent to a fluid system to the partition function

Thermodynamic variables for a fluid		
First law: $dU = TdS - PdV$		
Partition function		
$Z(T, V) = \sum_i e^{-\beta E_i}$		
↓		
Free energy		
$\mathcal{F} = -kT \ln Z$		
↙	↓	↘
Internal energy	Entropy	Pressure
$U = -\frac{\partial \ln Z}{\partial \beta}$	$S = -\left(\frac{\partial \mathcal{F}}{\partial T}\right)_V$ $= (U - \mathcal{F})/T$	$P = -\left(\frac{\partial \mathcal{F}}{\partial V}\right)_T$
↓	↓	↓
Specific heat (constant V)	Specific heat (constant $X = V, P$)	Isothermal compressibility
$C_V = \left(\frac{\partial U}{\partial T}\right)_V$	$C_X = T \left(\frac{\partial S}{\partial T}\right)_X$	$\kappa_T = -\frac{1}{V} \left(\frac{\partial V}{\partial P}\right)_T$

to the function \mathcal{F} defined in Section 2.1. To see this we recall that the thermodynamic definition of \mathcal{F} is

$$\mathcal{F} = U - TS. \quad (2.5)$$

Differentiating and using eqn (2.3)

$$d\mathcal{F} = dU - TdS - SdT = -MdH - SdT. \quad (2.6)$$

Hence $\mathcal{F} \equiv \mathcal{F}(H, T)$. (It may avoid some confusion to note that if the alternative form of the first law (eqn 2.4) is used the free energy defined by eqn (2.5) becomes a function of M and T . This convention is used in some texts.)

2.3 Convexity properties of the free energy

A function $f(x)$ is a convex function of its argument x if

$$f\left(\frac{x_1 + x_2}{2}\right) \leq \frac{f(x_1) + f(x_2)}{2} \quad (2.7)$$

for all x_1 and x_2 . If the inequality sign is reversed the function is said to be concave. A more useful definition for our purposes is that if the second derivative exists it must be ≥ 0 for a convex function and ≤ 0 for a concave function.

To determine the convexity properties of the free energy consider its second derivatives

$$\left(\frac{\partial^2 \mathcal{F}}{\partial T^2}\right)_H = \frac{-C_H}{T}, \quad \left(\frac{\partial^2 \mathcal{F}}{\partial H^2}\right)_T = -\chi_T \quad (2.8)$$

where C_H is the specific heat at constant field and χ_T is the isothermal susceptibility. It follows from the third law of thermodynamics that specific heats must be non-negative. Susceptibilities are usually positive, but there are exceptions, such as diamagnetic materials. However, it can be proved that if the Hamiltonian can be written

$$\mathcal{H} = \mathcal{H}_0 - HM \quad (2.9)$$

they must be positive³. This formula will apply to all the cases which will be considered here. Because the second derivatives of the free

³ Griffiths, R. B. (1965). *Journal of Chemical Physics*, **43**, 1958.

energy with respect to T and H are negative it is a concave function of both its variables.

2.4 Correlation functions

Thermodynamic variables like the magnetization or the entropy are macroscopic properties. In Section 1.2 it became apparent that a much fuller understanding of phase transitions could be obtained by considering what was happening on a microscopic level. To be able to do this in a more quantitative way we introduce correlation functions. For example the spin-spin correlation function, defined to measure the correlation between the spins on sites i and j , is

$$\Gamma(\vec{r}_i, \vec{r}_j) = \langle (s_i - \langle s_i \rangle)(s_j - \langle s_j \rangle) \rangle \quad (2.10)$$

where \vec{r}_i is the position vector of site i and $\langle \dots \rangle$ denotes a thermal average. If the system is translationally invariant $\langle s_i \rangle = \langle s_j \rangle$ and Γ depends only on $(\vec{r}_i - \vec{r}_j)$

$$\Gamma(\vec{r}_i - \vec{r}_j) \equiv \Gamma_{ij} = \langle s_i s_j \rangle - \langle s \rangle^2. \quad (2.11)$$

Away from the critical point the spins become uncorrelated as $r \rightarrow \infty$ and hence the correlation function decays to zero. Note that this is true not only above but also below the critical temperature, although here the mean value of the spin $\langle s \rangle \neq 0$, because, as is evident from eqn (2.10), the correlations are measured between the fluctuations of the spins away from their mean values. The correlations decay to zero exponentially with the distance between the spins

$$\Gamma(r) \sim r^{-\tau} \exp^{-r/\xi} \quad (2.12)$$

where τ is some number. Equation (2.12) provides a definition of the correlation length, ξ , which was used in Section 1.2 as an estimate of the size of the largest ordered clusters in the Monte Carlo generated snapshots of an Ising model. We have assumed that ξ is independent of the direction of \vec{r} . This is usually the case for large r near criticality.

At the critical point itself long-range order develops in the system. The correlation length becomes infinite and eqn (2.12) breaks down. Evidence from experiments and exactly soluble models shows that here the correlation function decays as a power law

$$\Gamma(r) \sim \frac{1}{r^{d-2+\eta}} \quad (2.13)$$

where η , our first example of a critical exponent, is a system-dependent constant⁴.

It is possible to relate the spin-spin correlation function to the fluctuations in the magnetization and hence to the susceptibility. Using the formula relating the magnetization to the partition function given in Table 2.1 one can check that the fluctuations in the magnetization are given by

$$\langle (M - \langle M \rangle)^2 \rangle = \langle M^2 \rangle - \langle M \rangle^2 = k^2 T^2 \frac{\partial^2}{\partial H^2} \ln \mathcal{Z} = kT \chi_T. \quad (2.14)$$

But, writing the magnetization as a sum over spins,

$$\langle (M - \langle M \rangle)^2 \rangle = \sum_i \langle (s_i - \langle s_i \rangle) \sum_j (s_j - \langle s_j \rangle) \rangle = \sum_{ij} \Gamma_{ij}. \quad (2.15)$$

For a translationally invariant system

$$\sum_{ij} \Gamma_{ij} = N \sum_i \Gamma_{i0} \sim N \int \Gamma(r) r^{d-1} dr \quad (2.16)$$

where the sum has been replaced by an integral, a step justified near criticality where the lattice structure is unimportant. Combining eqns (2.14), (2.15), and (2.16) we obtain

$$\chi_T \sim N \int \Gamma(r) r^{d-1} dr. \quad (2.17)$$

At the critical temperature the susceptibility diverges and hence $\Gamma(r)$ must become sufficiently long range that the integral on the right hand side of eqn (2.17) also diverges. This sets an upper limit on η (2. Note, from eqn (2.14), that a divergent susceptibility also implies divergence in the fluctuations of the magnetization.

2.5 First-order and continuous phase transitions

A phase transition is signalled by a singularity in a thermodynamic potential such as the free energy. If there is a finite discontinuity one or more of the first derivatives of the appropriate thermodynamic potential the transition is termed first-order. For a magnetic system the free energy \mathcal{F} , defined by eqn (2.5), is the appropriate potential

⁴Fisher, M. E. (1964). *Journal of Mathematical Physics*, 5, 944.

with a discontinuity in the magnetization showing that the transition is first-order. For a fluid the Gibbs free energy, $G = \mathcal{F} + PV$, is relevant and there are discontinuities in the volume and the entropy across the vapour pressure curve. A jump in the entropy implies that the transition is associated with a latent heat.

If the first derivatives are continuous but second derivatives are discontinuous or infinite the transition will be described as higher order, continuous, or critical⁵. This type of transition corresponds to a divergent susceptibility, an infinite correlation length, and a power law decay of correlations (eqn 2.13).

It will be helpful to look more carefully at how the thermodynamic variables behave near a phase transition for a particular case. The aim is to compare the behaviour at first- and higher order transitions and to look in some detail at the signatures of the latter with a view to defining the critical exponents in Section 2.6.

The example is the simple ferromagnet in a magnetic field. Its phase diagram was introduced in Chapter 1 and is reproduced for convenience in Fig. 2.1(a). There is a line of first-order transitions at zero field stretching from zero temperature to end at a critical point at a temperature $T = T_c$. The symmetry of the phase diagram, which is a consequence of the symmetry of a ferromagnet under reversal of the magnetic field, does not obscure any salient features. An example of a case where this symmetry is missing is the liquid-gas transition depicted in Fig. 1.1.

We first describe the field dependence of the free energy and its field derivatives, the magnetization and the susceptibility, along the three paths 1, 2, and 3 in Fig. 2.1(a). The aim is to compare the behaviour of these functions at temperatures below, equal to, and above T_c .

The free energy itself is shown in Fig. 2.1(b). Note that it is convex and symmetric about $H = 0$ as expected. A cusp develops at $H = 0$ for $T < T_c$. This signals a first-order phase transition as is seen more clearly in the behaviour of the magnetization, M .

The variation of M with H is shown in Fig. 2.1(c). For $T > T_c$ it varies continuously. For $T < T_c$, however, there is a jump at zero field indicative of the first-order phase transition. At the temperature di-

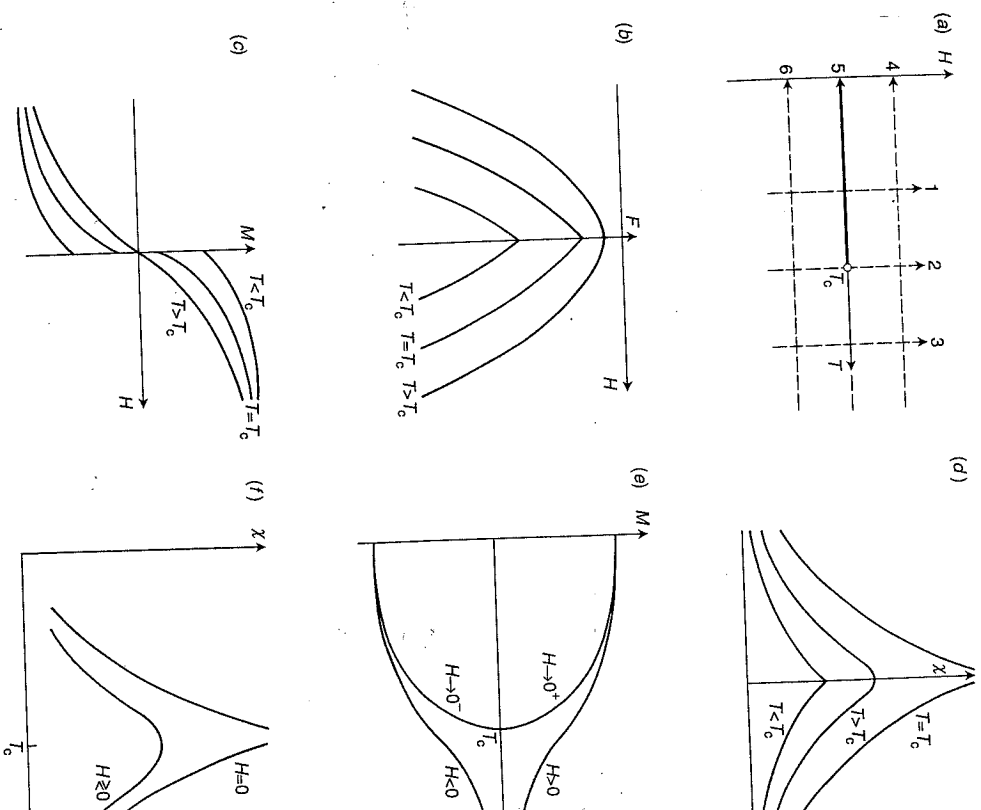


Fig. 2.1. (a) Phase diagram of a simple ferromagnet. There is a line of first-order transitions along $H = 0$ which ends at a critical point at $T = T_c$. (b) Field dependence of the free energy. (c) Field dependence of the magnetization. (d) Field dependence of the magnetization. (e) Temperature dependence of the magnetization. (f) Temperature dependence of the susceptibility.

⁵The term 'second-order' phase transition, used synonymously with continuous phase transition, is a relic of the original classification of phase transitions into first-, second-, third-... order due to Ehrenfest. This essentially recognized only discontinuities in thermodynamic derivatives, rather than divergences, which has been proved inappropriate. Therefore we follow M. E. Fisher in terming transitions first-order or continuous.

viding these behaviours, the critical temperature T_c , the magnetization is continuous at $H = 0$ but has infinite slope.

Differentiating again one obtains the isothermal susceptibility χT , which behaves in a definitive way at the critical temperature. The susceptibility is plotted as a function of field in Fig. 2.1(d). For $T > T_c$ it is a smooth function of the field as expected. Below T_c the susceptibility has a cusp at the first-order phase transition, $H = 0$. At the critical point itself the susceptibility diverges, a behaviour characteristic of a continuous phase transition.

We shall also be interested in how the magnetization and the susceptibility vary with temperature at constant field. This can be inferred from Figs 2.1(c) and 2.1(d) for the three paths 4, 5, and 6 in Fig. 2.1(a). Note that because of the symmetry of the magnetic phase diagram it is not possible to cross a line of first-order transitions by varying the temperature as would be the case generically. Following path 5 at $H = 0$ one passes through T_c and then follows a line of two-phase coexistence to zero temperature. Along paths 4 and 6, which have been chosen to lie equidistant from $H = 0$ to display the symmetry of the model better, there is no phase transition.

The temperature dependence of the magnetization is shown in Fig. 2.1(e). For non-zero field the magnetization increases smoothly with decreasing temperature to attain its saturation value, corresponding to all the spins being aligned, at zero temperature. The spins align along the direction of the field; if $H > 0$ the magnetization is positive and vice versa.

For $H = 0$ no preferred direction is singled out by the field and, for $T > T_c$, correlated regions of spins are finite and equally likely to point up or down. Hence the net magnetization is zero. At the critical temperature the correlation length becomes infinite, allowing a single cluster to dominate and a non-zero magnetization. The magnetization increases from zero at $T = T_c$ to its saturation value at $T = 0$. States with positive or negative magnetization have identical free energies. The two branches of the zero-field magnetization curve in Fig. 2.1(e) reflect this. The upper curve would be attained the presence of an infinitesimally small positive field; the curve corresponding to negative magnetization in an infinitesimally small negative field. Alternatively, cooling in a field and then taking the limit $H \rightarrow 0^+$ or $H \rightarrow 0^-$ would give positive or negative M respectively.

Finally we plot in Fig. 2.1(f) the susceptibility as a function of temperature. It must follow from symmetry that the susceptibility depends only on the magnitude of H , not on its sign. For finite field there is a peak in the susceptibility at T_c . For $H = 0$ this becomes a divergence signalling the critical point.

2.6 Critical point exponents

We have considered the dependence of the free energy on H and of its derivatives with respect to the field, the magnetization, and the susceptibility, on H and T . What about the temperature dependence of the free energy? For non-zero field there is no phase transition and hence the free energy is an analytic function of the temperature. For $H = 0$ one passes through a critical point as the temperature is lowered. This shows up in the second derivatives of the free energy.

Finally, for completeness, we mention the behaviour of the temperature derivatives of the free energy, the entropy, and the specific heat. At a first-order transition there is a usually a jump in the entropy and hence a latent heat⁶. The existence of a critical point is often marked by a specific heat which diverges at the critical temperature. An example of this is shown in Fig. 1.3.

2.6 Critical point exponents

We have argued that the critical point is marked by divergences in the specific heat and the susceptibility. It turns out to be very important to the theory of critical phenomena to understand more carefully the form of these divergences and the singular behaviour of the other thermodynamic functions near the critical point. To do this we define a set of critical exponents. We shall then start to justify why they play such a central role in the theory of critical phase transitions.

Let $t = (T - T_c)/T_c$ (2.18)

be a measure of the deviation in temperature from the critical temperature T_c . Then the critical exponent associated with a function $F(t)$ is⁷

$$\lambda = \lim_{t \rightarrow 0} \frac{\ln |F(t)|}{\ln |t|} \quad (2.19)$$

or, as it is more usually written,

$$F(t) \sim |t|^\lambda. \quad (2.20)$$

The \sim sign is well advised as it is important to remember that eqn (2.20) only represents the asymptotic behaviour of the function $F(t)$ as $t \rightarrow 0$. More generally one might expect

⁶For the ferromagnet the transition is between states of magnetization opposite in sign but equal in magnitude. Hence this is a transition with no associated latent heat.

⁷Assuming that the limit exists. See problem 2.3 for an example where this is not the case.

Table 2.3. Definitions of the most commonly used critical exponents for a magnetic system

Zero-field specific heat	$C_H \sim t ^{-\alpha}$
Zero-field magnetization	$M \sim (-t)^\beta$
Zero-field isothermal susceptibility	$\chi_T \sim t ^{-\gamma}$
Critical isotherm ($t = 0$)	$H \sim M ^\delta \operatorname{sgn}(M)$
Correlation length	$\xi \sim t ^{-\nu}$
Pair correlation function at T_c	$G(r) \sim 1/r^{d-2+\eta}$

$$F(t) = A |t|^\lambda (1 + bt^{\lambda_1} + \dots), \quad \lambda_1 > 0. \quad (2.21)$$

To check that this is a reasonable way of describing the leading behaviour of the singularities in the thermodynamic functions consider the zero-field magnetization of a ferromagnet shown in Fig. 2.1(e). Near T_c a sensible guess would be to describe the curve by a formula $M \sim (-t)^\beta$ with $\beta \sim 1/2$ because of the resemblance to a parabola.

The zero-field susceptibility diverges at T_c as shown in Fig. 2.1(f) and the zero-field specific heat shows qualitatively similar behaviour. Hence we may write

$$\chi_T \sim |t|^{-\gamma}; \quad C_H \sim |t|^{-\alpha} \quad (2.22)$$

where α and γ are positive.

A fourth exponent, δ , is introduced to describe the behaviour of the critical isotherm near the critical point at $H = 0$,

$$H \sim |M|^\delta \operatorname{sgn}(M) \quad (T = T_c). \quad (2.23)$$

Check that this corresponds to a curve of the form shown in Fig. 2.1(c). One might guess $\delta \sim 2$.

The critical exponent definitions are collected together in Table 2.3 for a magnetic system and Table 2.4 for a fluid. η and ν are associated with the pair correlation function and correlation length which were defined in Section 2.4. In particular, ν describes how the correlation length diverges as the critical temperature is approached.

Table 2.4. Definitions of the most commonly used critical exponents for a fluid system

Specific heat at constant volume V_c	$C_V \sim t ^{-\alpha}$
Liquid-gas density difference	$(\rho_l - \rho_g) \sim (-t)^\beta$
Isothermal compressibility	$\kappa_T \sim t ^{-\gamma}$
Critical isotherm ($t = 0$)	$P - P_c \sim \rho_l - \rho_g ^\delta \operatorname{sgn}(\rho_l - \rho_g)$
Correlation length	$\xi \sim t ^{-\nu}$
Pair correlation function at T_c	$G(r) \sim 1/r^{d-2+\eta}$

In compiling Tables 2.3 and 2.4 we have made the as yet totally unjustified assumption that the critical exponent associated with a given thermodynamic variable is the same as $T \rightarrow T_c$ from above or below. Early series and numerical work suggested that this was the case, but it was only with the advent of the renormalization group that it was indeed proved to be so. A common notation was to use a prime to distinguish the value of an exponent as $T \rightarrow T_c^-$ from the value as $T \rightarrow T_c^+$.

2.6.1 Universality

Having defined the critical exponents we need to justify why they are interesting. And indeed, why they are more interesting than the critical temperature T_c itself. It turns out that, whereas T_c depends sensitively on the details of the interatomic interactions, the critical exponents are to a large degree *universal* depending only on a few fundamental parameters. For models with short-range interactions these are the dimensionality of space, d , and the symmetry of the order parameter.

Striking evidence for this comes from a plot by Guggenheim presented as long ago as 1945. This is shown in Fig. 2.2 where the coexistence curves of eight different fluids are plotted in reduced units, T/T_c and ρ/ρ_c . Close to the critical point (and indeed surprisingly far away from it!) all the data lie on the same curve and hence can be described by the same exponent β . The fit assumes $\beta = 1/3$.

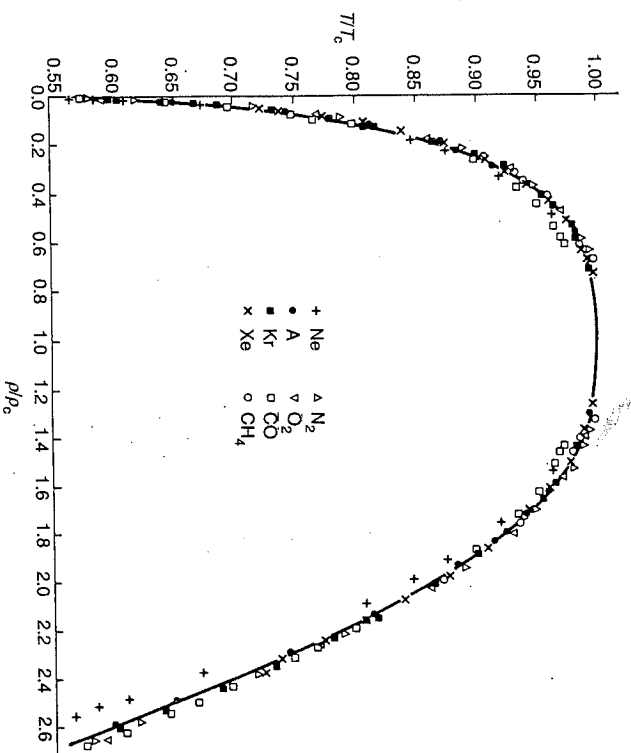


Fig. 2.2. The coexistence curve of eight different fluids plotted in reduced variables. The fit assumes an exponent $\beta = 1/3$. After Guggenheim, E. A. (1945). *Journal of Chemical Physics*, 13, 253.

A further test of universality is to compare this value to that obtained for a phase transition in a completely different system with a scalar order parameter. Magnets with uniaxial anisotropy in spin space are one possibility—for MnF_2 a classic experiment by Heller and Benedek⁸ gave $\beta = 0.335(5)$ where the number in brackets denotes the uncertainty in the final decimal place. For phase separation in the binary fluid mixture $\text{CCl}_4 + \text{C}_7\text{F}_{16}$ the experimental result⁹ is $\beta = 0.33(2)$.

The Ising model, which we introduced as a simple example of an interacting system in Section 1.2 also has a scalar order parameter. It cannot be solved exactly in three dimensions but numerical estimates of the values of the critical exponents are very precise and provide a stringent test of universality. For the simple cubic, body-centred cubic, and face-centred cubic lattices $K_c = kT_c/J = 0.2216, 0.1574,$ and 0.1021 respectively. However, in all three cases β is the same, 0.327 , with some argument about the value of the last decimal place¹⁰.

This immediately illustrates the power of using simple models to describe critical behaviour. By making sure that one is working in the right dimension and that the symmetry of the order parameter is correctly represented by a model, it can be used to obtain critical exponents for all the systems within its universality class. It is much easier to study the Ising model than a complicated fluid Hamiltonian belonging to them. Therefore a discussion of other universality classes will be postponed to the next chapter when we will have defined the relevant models.

2.6.2 Exponent inequalities

It is possible to obtain several rigorous inequalities between the critical exponents. The easiest to prove is due to Rushbrooke. It follows from the well known thermodynamic relation between the specific heats a constant field and constant magnetization

$$\chi T(C_H - C_M) = T \left(\frac{\partial M}{\partial T} \right)_H^2 \quad (2.22)$$

Because C_M must be greater than or equal to zero,

⁸Heller, P. and Benedek, G. B. (1962). *Physical Review Letters*, 428.

⁹Thompson, D. R. and Rice, O. K. (1964). *Journal of the American Chemical Society*, 86, 3547.

¹⁰Lin, A. J. and Fisher, M. E. (1989). *Physica*, A156, 35.

$$C_H \geq T \left(\frac{\partial M}{\partial T} \right)_H^2 / \chi_T. \quad (2.25)$$

As $t \rightarrow 0^-$ in zero field, using the definitions of the critical exponents in Table 2.3,

$$C_H \sim (-t)^{-\alpha}, \quad \chi_T \sim (-t)^{-\gamma}, \quad \left(\frac{\partial M}{\partial T} \right)_H \sim (-t)^{\beta-1}. \quad (2.26)$$

Therefore the inequality (2.25) can only be obeyed if

$$\alpha + 2\beta + \gamma \geq 2. \quad (2.27)$$

Other inequalities, for example

$$\alpha + \beta(1 + \delta) \geq 2, \quad (2.28)$$

can be obtained from the convexity properties of the free energy. Yet others, for example

$$\gamma \leq (2 - \eta)\nu; \quad d\nu \geq 2 - \alpha; \quad \gamma \geq \beta(\delta - 1), \quad (2.29)$$

follow from making reasonable assumptions about the behaviour of the thermodynamic variables or correlation functions¹¹.

For the two-dimensional Ising model $\alpha = 0$, $\beta = 1/8$, $\gamma = 7/4$, $\delta = 15$, $\nu = 1$, and $\eta = 1/4$ and one can check that all the inequalities listed above actually hold as equalities. Exponents for some other universality classes are given in Table 3.1 and the reader might like to check whether the scaling laws are obeyed as equalities for these.

We have introduced two very new ideas, universality and inequalities between the critical exponents which appear to hold as equalities. The reader might well be demanding to know why the exponents have these striking properties. Such an explanation, based on the physics of scale invariance, will be forthcoming in Chapter 8 when the renormalization group is described. In the intervening chapters we look in more detail at models of systems which undergo phase transitions and how to calculate their critical exponents and other properties.

¹¹The derivation of these inequalities is discussed in Stanley, H. E. (1971), *Introduction to phase transitions and critical phenomena*, Ch. 4. (Oxford University Press, Oxford).

2.7 Problems

2.1 (i) Verify eqn (2.14).

(ii) Show in a similar way that the fluctuations in the energy are related to the specific heat at constant volume by

$$(\Delta E)^2 \equiv ((E - \langle E \rangle)^2) = kT^2 C_V.$$

Use this equation to argue that $\Delta E \sim N^{1/2}$ where N is the number of particles in the system.

2.2 A paramagnetic solid contains a large number N of non-interacting, spin-1/2 particles, each of magnetic moment μ on fixed lattice sites. This substance is placed in a uniform magnetic field H .

(i) Write down an expression for the partition function of the solid, neglecting lattice vibrations, in terms of $x = \mu H/kT$.

(ii) Find the magnetization M , the susceptibility χ , and the entropy S , of the paramagnet in the field H .

(iii) Check that your expressions have sensible limiting forms for $x \gg 1$ and $x \ll 1$. Describe the microscopic spin configuration in each of these limits.

(iv) Sketch M , χ , and S as a function of x .

[Answers: (i) $Z = (2 \cosh x)^N$; (ii) $M = N\mu \tanh x$, $\chi = N\mu^2/(kT \cosh^2 x)$, $S = Nk\{\ln 2 + \ln(\cosh x) - x \tanh x\}$]

2.3 Determine the critical exponents λ for the following functions as $t \rightarrow 0$:

- | | |
|-------|-----------------------------------|
| (i) | $f(t) = At^{1/2} + Bt^{1/4} + Ct$ |
| (ii) | $f(t) = At^{-2/3}(t + B)^{2/3}$ |
| (iii) | $f(t) = At^2 e^{-t}$ |
| (iv) | $f(t) = At^2 e^{1/t}$ |
| (v) | $f(t) = A \ln\{\exp(1/t^4) - 1\}$ |

[Answers: (i) 1/4, (ii) -2/3, (iii) 2, (iv) undefined, (v) -4.]

2.4 Show that the following functions have a critical exponent $\lambda = 0$ in the limit $t \rightarrow 0$:

- | | |
|-------|--|
| (i) | $f(t) = A \ln t + B$ |
| (ii) | $f(t) = A - Bt^{1/2}$ |
| (iii) | $f(t) = 1, t < 0; \quad f(t) = 2, t > 0$ |
| (iv) | $f(t) = A(t^2 + B^2)^{1/2} \ln t ^2$ |
| (v) | $f(t) = At \ln t + B$ |

2.5¹² Consider a model equation of state that can be written

$$H \sim aM(t + bM^2)^\theta; \quad 1 < \theta < 2; \quad a, b > 0.$$

near the critical point. Find the exponents β , γ , and δ and check that they obey the inequality given in (2.29) as an equality.

[Answer: $\beta = 1/2$, $\gamma = \theta$, $\delta = 1 + 2\theta$]

2.6¹² The spontaneous magnetization per spin of the spin-1/2 Ising model on the square lattice is

$$\langle s \rangle^8 = 1 - (\sinh 2J/kT)^{-4}.$$

Show that this can be written in the form

$$\langle s \rangle = B(-t)^\beta \{1 + b(-t) \dots\}$$

where $t = (T - T_c)/T_c$ and $\beta = 1/8$. Find B and b and hence estimate the range of temperatures over which it is reasonable to ignore the correction to the leading scaling behaviour.

[Answer: $B = (8\sqrt{2}K_c)^{1/8}$, $b = (1 - 9K_c/\sqrt{2})/8$ where $K_c = J/kT_c$.]

3

Models

The aim of this chapter is to describe some of the most fundamental models of cooperative behaviour. To model a physical system one route is to include, as realistically as possible, all the complicated many body interactions and try to obtain a quantitative prediction of the behaviour by solving Schrödinger's equation numerically. The other extreme is to write down the simplest possible model that still includes the essential physics and hope that it is tractable to analytic or precise numerical solution. The aim here is often to study universal behaviour or to gain a qualitative understanding of the physics governing the behaviour of a given class of materials.

It is the latter approach that we shall take here. Despite the apparent simplicity of the models, they show a rich mathematical structure and are in general difficult or, more usually, impossible to solve exactly. Moreover, and perhaps surprisingly at first sight, they do provide valid and useful representations of experimental systems. We shall return to discuss why this should be the case at the end of the chapter when armed with concrete examples.

It is conventional and convenient to use magnetic language and write the model Hamiltonians in terms of spin variables, although they will turn out to be applicable to many non-magnetic systems. In all the examples considered here the spins will lie on the sites i of a regular lattice. Three-dimensional lattices, such as simple cubic, body-centred cubic, and face-centred cubic, are familiar from conventional crystallography but we shall also be interested in lattices in two dimensions, such as the square, triangular, and hexagonal lattices shown in Fig. 3.1, and in one dimension where the lattice is just a linear chain of sites. It will become apparent in later chapters that most of the scientists in this field show a marked preference for working in any dimension but three.

¹² After M. E. Fisher.

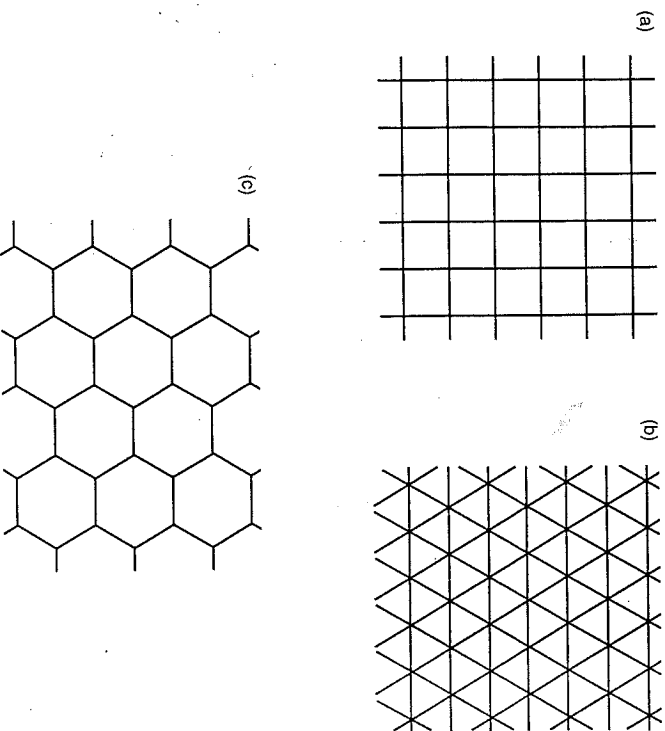


Fig. 3.1. Examples of two-dimensional regular lattices (a) square, (b) triangular, (c) hexagonal.

3.1 The spin-1/2 Ising model

A remarkably successful model of an interacting system, and one that we shall use continually as an example throughout this book, is the spin-1/2 Ising model. A classical spin variable s_i , which is allowed to take values ± 1 , is placed on each lattice site. The spins interact according to a Hamiltonian

$$\mathcal{H} = -J \sum_{\langle ij \rangle} s_i s_j - H \sum_i s_i. \quad (3.1)$$

The first term in eqn (3.1) is responsible for the cooperative behaviour and the possibility of a phase transition. J is the exchange energy: positive J favours parallel and negative J antiparallel alignment of the spins. We shall use $\langle ij \rangle$ to denote a sum over nearest neighbour spins; further-neighbour interactions and terms which involve more than two spins can be added to the Hamiltonian at will.

For $J = 0$, eqn (3.1) is the Hamiltonian of a paramagnet. A discussion of its statistical mechanics forms an early chapter in elementary statistical mechanics texts. The only influence ordering the spins is the field H . They do not interact, there are no cooperative effects and hence no phase transition.

The Ising model is not difficult to solve in one dimension and we shall do so (several times) as an example of the use of transfer matrices, series expansions and the renormalization group. However, one dimension represents a special case because the phase transition is at zero temperature.

The calculation of the exact partition function of the two-dimensional Ising model in zero field was a mathematical *tour de force* performed by Onsager in 1944. Extensions of his work mean that values are now known for all the critical exponents—they are rational fractions in two dimensions for reasons that remained obscure for a long time. The two-dimensional Ising model in a magnetic field and the three-dimensional model, even in zero field, remain unsolved although their properties are known very precisely from numerical work. Professor K. G. Wilson, who won the Nobel prize in 1982 for his work on the renormalization group, describes:

When I entered graduate school I had carried out the instructions given to me by my father and had knocked on both Murray Gell-Mann's and Feynman's doors and asked them what they were currently doing. Murray wrote down the partition function for the three-dimensional Ising model and said it would be nice if I could solve it (at least that is how I remember the conversation). Feynman's answer was 'nothing'.

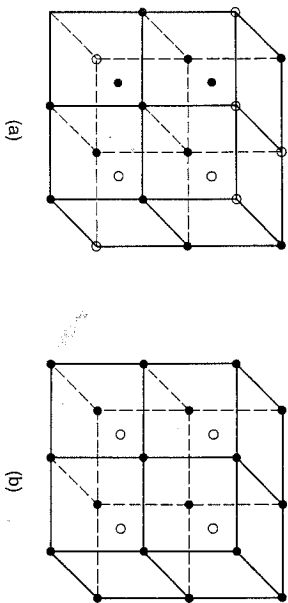


Fig. 3.2. A typical configuration of the copper and zinc atoms of beta-brass on the body-centred cubic lattice: (a) $T \gg T_c$; (b) $T \ll T_c$.

Despite its simplicity the Ising model is widely applicable because it describes any interacting two-state system. We illustrate this with two examples.

3.1.1 Order-disorder transitions in binary alloys

A classical example of a binary alloy is beta-brass. Beta-brass consists of equal numbers of copper and zinc atoms which lie on the sites of a body-centred cubic lattice. At high temperatures each lattice site is occupied at random by a copper or zinc atom giving the disordered structure shown in Fig. 3.2(a). We stress that the disorder is substitutional—the atoms occupy random positions on the lattice—rather than topological—the lattice itself has not ceased to exist, as would be the case for a liquid.

As the temperature is lowered there is, at $T_c = 733\text{K}$, a continuous phase transition to an ordered state where each atomic species preferentially occupies one of the two sublattices of the body-centred cubic lattice. The atomic configuration for $T \ll T_c$ is shown in Fig. 3.2(b). A suitable order parameter is the difference between the number of copper and zinc atoms on a chosen sublattice. Its variation with temperature is shown in Fig. 3.3.

Our aim is to write down a Hamiltonian which describes the interactions in beta-brass and predicts a continuous phase transition. To this end we assign the variables

$$s_i = 1 \text{ if site } i \text{ is occupied by a copper atom,}$$

$$s_i = -1 \text{ if site } i \text{ is occupied by a zinc atom.}$$

The spin on each site can take two values and hence is a spin-1/2 Ising variable. Defining J_{CuCu} , J_{ZnZn} and J_{CuZn} as the interaction

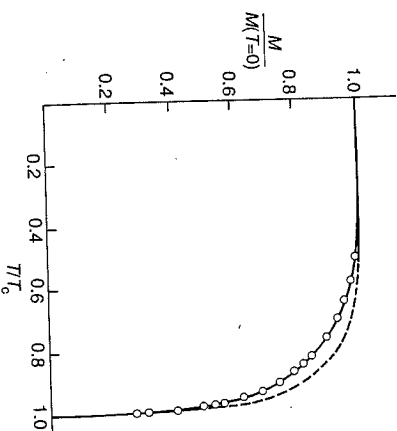


Fig. 3.3. Temperature dependence of the order parameter of beta-brass. The open circles are neutron scattering results, the dashed line X-ray scattering results, and the full line is the theoretical result for a compressible Ising model. The discrepancy between the X-ray and neutron data may arise because of the low sensitivity of X-rays to the atomic ordering. After Als-Nielsen, J. (1976). Neutron scattering and spatial correlation near the critical point. In *Phase transitions and critical phenomena*, Vol. 5a (eds C. Domb and M. S. Green), p.87. (Academic Press, London).

between two copper atoms, two zinc atoms, and a copper and a zinc atom respectively we may write the Hamiltonian

$$\mathcal{H} = \frac{1}{4} \sum_{\langle ij \rangle} J_{CuCu} (1 + s_i)(1 + s_j) + \frac{1}{4} \sum_{\langle ij \rangle} J_{ZnZn} (1 - s_i)(1 - s_j) + \frac{1}{4} \sum_{\langle ij \rangle} J_{CuZn} \{ (1 + s_i)(1 - s_j) + (1 - s_i)(1 + s_j) \}. \quad (3.2)$$

It is easy to check that if sites i and j are both occupied by copper atoms so that $s_i = s_j = 1$ this reduces to J_{CuCu} and so on. Collecting terms in eqn (3.2) gives

$$\mathcal{H} = -J \sum_{\langle ij \rangle} s_i s_j - H \sum_i s_i + C \quad (3.3)$$

where $J = \frac{1}{4}(J_{CuCu} + J_{ZnZn} - 2J_{CuZn})$, C is a spin-independent term, and, because there are equal numbers of copper and zinc atoms, $\sum_i s_i = 0$.

We have arrived at the Hamiltonian of the nearest-neighbour spin-1/2 Ising model on a body-centred cubic lattice in zero field. What approximations are inherent in using this to describe beta-brass? Firstly I should like to stress that the use of an Ising variable is not an approximation (as long as there are no impurities or vacancies) as each lattice site is strictly in one of two states, occupied by copper or occupied by zinc. Therefore, because of the ideas of universality, the exponents should be those of the three-dimensional Ising model even if the details of the interatomic interactions are not well described by the Hamiltonian (3.2). This is borne out by the experimental values $\beta = 0.305 \pm 0.005$ and $\gamma = 1.24 \pm 0.015^1$ which should be compared to the current best estimates for the three-dimensional Ising model $\beta \approx 0.33$ and $\gamma \approx 1.24$.

To go beyond universal properties and try to predict experimental results like the variation of the order parameter with temperature the details of the interactions included in the model Hamiltonian become important. In general, further-neighbour interactions and multi-spin

¹Als-Nielsen, J. (1976). Neutron scattering and spatial correlation near the critical point. In *Phase transitions and critical phenomena*, Vol. 5a (eds C. Domb and M. S. Green), p.87. (Academic Press, London). The discrepancy in β is thought to result from the thermal expansion of the lattice affecting the temperature dependence of the order parameter near criticality.

terms (such as $s_i s_j s_k$) and long-range interactions must be included to reproduce the thermodynamic functions correctly. In this particular example, however, they turn out to be unimportant. For beta-brass the most significant correction to the Ising model result comes from the variation of the exchange interaction J with temperature which results from the thermal expansion of the lattice. Allowing for this, the agreement with experiment is excellent, as shown in Fig. 3.3.

3.1.2 Lattice gas models

The archetypal lattice gas is a model where each lattice site can either be occupied by an atom or vacant. A variable $t_i = 1, 0$ is used to represent an occupied or unoccupied site respectively. The Hamiltonian is

$$\mathcal{H} = -J_L \sum_{\langle ij \rangle} t_i t_j - \mu_L \sum_i t_i \quad (3.4)$$

where J_L is a nearest neighbour interaction which favours neighbouring sites being occupied. μ_L is a chemical potential which controls the number of atoms: a large positive μ_L will lead to most sites being occupied whereas a large negative μ_L will favour vacancies.

As t_i is a two-state variable it must be possible to map it on to a Ising spin, $s_i = \pm 1$. This is achieved by the transformation

$$t_i = (1 - s_i)/2. \quad (3.5)$$

Substituting eqn (3.5) into eqn (3.4) one regains the usual nearest neighbour, spin-1/2 Ising Hamiltonian with the field related to the chemical potential.

A system which is well modelled by a lattice gas and which also illustrates the possibility of realizing experimental examples of the Ising model in two dimensions is hydrogen adsorbed on the (110) surface of iron. The atomic configuration of a (110) plane of iron is shown in Fig. 3.4(a). The potential wells between the iron atoms form a triangular lattice and define possible sites for the adsorption of hydrogen. Each site can either be occupied ($t_i = 1$) or vacant ($t_i = 0$) with a number of occupied sites, or coverage, being determined by the pressure of the hydrogen gas in contact with the surface.

As each adsorption site can be either occupied or vacant it has states, and hence the phases of hydrogen on iron should be amenable to description by a lattice gas or equivalently an Ising model. As coverage is varied several different ordered phases exist as the equilibrium state of the adsorbed hydrogen atoms. Some of these are shown in Fig. 3.4(b). They cannot be described by an Ising model with

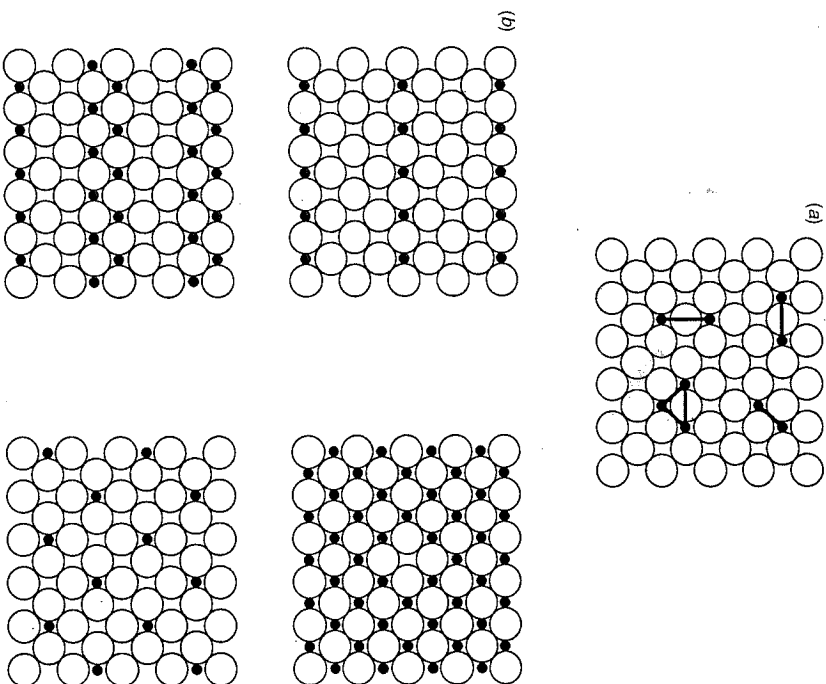


Fig. 3.4. (a) The atomic configuration of a (100) plane of iron showing the adsorption sites for the hydrogen atoms and the interactions included in a model Hamiltonian for this system. (b) Some of the resulting equilibrium phases.

nearest neighbour interactions, but by including the anisotropic second neighbour term and a three-spin interaction proportional to the product of spins around each elementary triangle shown in Fig. 3.4(a), three different phases and the transitions between them can be understood in some detail.

3.2 The spin-1 Ising model

For systems with more than two states higher-spin Ising models are appropriate. For example, the most general Hamiltonian for the spin-1 Ising model is

$$\mathcal{H} = -J \sum_{\langle ij \rangle} s_i s_j - K \sum_{\langle ij \rangle} s_i^2 s_j^2 - D \sum_i s_i^2 - L \sum_{\langle ij \rangle} (s_i^2 s_j + s_i s_j^2) - H \sum_i s_i, \quad s_i = \pm 1, 0. \quad (3.6)$$

This follows from allowing all possible terms $s_i^\alpha s_j^\beta$; $\alpha, \beta = 0, 1$, Higher powers of the spin do not enter because $s_i^3 = s_i$.

Because of its enlarged parameter space the spin-1 Ising model exhibits a much richer variety of critical behaviour than its spin-1/2 counterpart. The phase diagram for $K = L = 0$ is shown in Fig. 3.5. Three sheets of first order phase transitions join at a triple line where three phases coexist. The triple line ends in a tricritical point where the three phases become critical simultaneously.

3.3 The q -state Potts model

Many different spin models, some driven by theoretical and some experimental considerations, have been defined in the scientific literature. Several examples appear in the problems at the end of this and subsequent chapters. The only other classical spin model that I shall define here is the q -state Potts model. The relation of this system to the physicochemical description of krypton atoms on a graphite surface provides an interesting example of how to construct a model Hamiltonian with the correct symmetry.

To define the Potts model a q -state variable, $\sigma_i = 1, 2, 3, \dots, q$, is placed on each lattice site. The interaction between the spins is described by the Hamiltonian

$$\mathcal{H} = -J \sum_{\langle ij \rangle} \delta_{\sigma_i \sigma_j}. \quad (3.7)$$

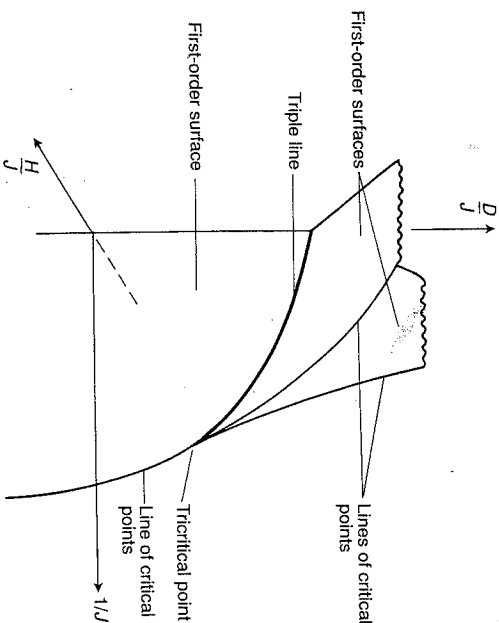


Fig. 3.5. A three-dimensional cross-section through the phase diagram of the spin-1 Ising model. Three surfaces of first-order transitions (two 'wings' and the lower portion of the $H = 0$ plane) meet at a triple line, shown in bolder type, where three phases coexist. The three phases become identical simultaneously at a tritcritical point which marks the end of the triple line or, equivalently, the point where the three lines of critical points bounding the first-order surfaces meet.

3.3

3.4

3.4 X-Y and Heisenberg models

δ is a Kronecker delta-function so the energy of two neighbouring spins is $-J$ if they lie in the same state and zero otherwise. It is easy to convince oneself that the Potts model has q equivalent ground states where all the spins are identical but can take any one of the q values. As the temperature is increased there is a transition to a paramagnetic phase which is continuous for $q \leq 4$ but first-order for $q > 4$ in two dimensions².

For $q = 2$ the Potts model is identical to the spin-1/2 Ising model. Note, however, that for $q = 3$ the Hamiltonian (3.7) does not correspond to the first term in eqn (3.6) because the three states of the spin-1 Ising model are not equivalent (see problem 3.2).

A physical realization of a system with the symmetry of the two-dimensional, three-state Potts model is krypton adsorbed on the basal planes of graphite. The surface of graphite comprises hexagonal rings of carbon atoms and it is favourable for an adsorbed krypton to lie within one of the rings. However, the krypton atoms are sufficiently big that once a hexagon is occupied it becomes unfavourable for an atom to lie on any neighbouring site. Therefore, for one third coverage, the krypton atoms form a triangular lattice as shown in Fig. 3.6. But there are three entirely equivalent positions for the lattice: on the sublattices labelled a, b, and c in the figure. Hence the system has the symmetry of the three-state Potts model where a site corresponds to a triplet of adsorption rings and $\sigma_i = 1, 2, 3$ to the possibilities of the adsorbed krypton lying on the a, b, or c sublattices respectively.

X-Y and Heisenberg models 43

We have so far ignored the most obvious application of a spin model to magnetic systems themselves. The restriction of the Ising model is that the spin vector can only lie parallel to the direction of quantization introduced by the magnetic field. This means that the Ising Hamiltonian can only prove useful in describing a magnet which is highly anisotropic in spin space. There are physical systems, MnF₂ for example, which to a good approximation obey this criterion, but fluctuations of the spin away from the axis of quantization must inevitably occur to some degree.

A more realistic model of many magnets with localized moment

$$\mathcal{H} = -J_z \sum_{\langle ij \rangle} s_i^z s_j^z - J_{\perp} \sum_{\langle ij \rangle} (s_i^x s_j^x + s_i^y s_j^y) - H \sum_i s_i^z \quad (3.8)$$

²Wu, F. Y. (1982). *Reviews of Modern Physics*, 54, 235.

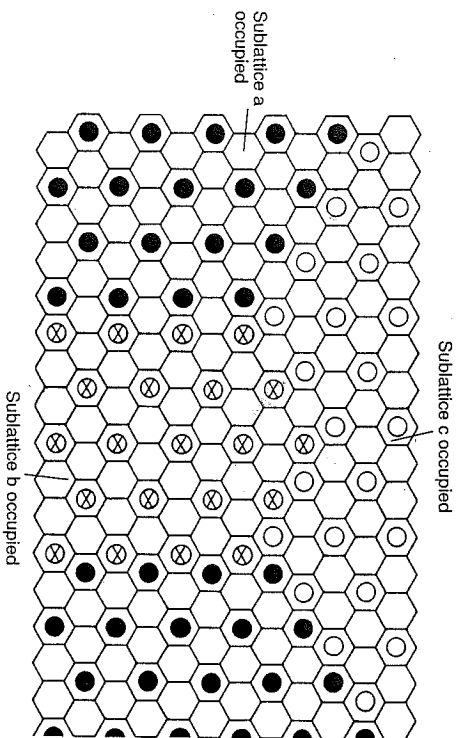


Fig. 3.6. Krypton adsorbed on the basal plane of graphite showing coexisting regions of the three ground states. After Kardar, M. and Berker, A. N. (1982). *Physical Review Letters*, **48**, 1552.

where x , y , and z label Cartesian axes in spin space. For $J_{\perp} = 0$ we regain the Ising model. For $J_z = J_{\perp}$ eqn (3.8) can be written

$$\mathcal{H} = -J \sum_{\langle ij \rangle} s_i^z s_j^z - H \sum_i s_i^z \quad (3.9)$$

This is the Heisenberg model.

The Heisenberg model was introduced in 1928 and was discussed in some detail as a model of ferromagnetism in Van Vleck's book of 1932³. It gives a reasonable description of the properties of some magnetic insulators, such as EuS, and provides a microscopic Hamiltonian describing the exchange interaction which leads to ferromagnetism. However, it does not include the possibility of non-localized spins and assumes complete isotropy in spin space.

The most fundamental theoretical difference between the Heisenberg and Ising models is that for the former the spin operators do not commute. Therefore it is a quantum mechanical rather than a classical

³Van Vleck, J. H. (1932). *The theory of electric and magnetic susceptibilities*. (Clarendon Press, Oxford).

spin model with corresponding greater difficulty in analytic or numerical treatments. Quantum models can be mapped on to classical spin systems in one higher dimension and there are some exact results for one-dimensional quantum models, just as for two-dimensional classical models⁴. Moreover, just as the Ising model only has a finite temperature phase transition for $d > 1$, the Heisenberg model orders at zero temperature unless $d > 2$.

The classical limit of the Heisenberg model can be constructed by taking the number of spin components to infinity and normalizing the spin from $\sqrt{S(S+1)}$ to 1. The spins become three-dimensional classical vectors. This limit, which leads to considerable simplifications in theoretical work, is useful because the critical exponents of the classical and quantum Heisenberg models are the same. This is an example of universality.

A second quantum mechanical spin model is the X-Y model, obtained by putting $J_z = 0$ in the Hamiltonian (3.8). This leads to spins which are two-dimensional, quantum mechanical vectors. The X-Y model, like the Heisenberg model, only has a conventional phase transition at non-zero temperature for $d > 2$. However, in $d = 2$ there is a transition at finite temperatures to an unusual ordered phase with a quasi long-range order. This is marked by the correlations decaying algebraically (as in eqn 2.13) for all temperatures, not just at the critical point itself⁵.

3.5 Universality revisited

In Section 2.6.1 the concept of the universality of critical exponents was described: that, for models with short-range interactions, the exponents depend only on the dimensionality of space and the symmetry of the order parameter. Several systems with the exponents of the three-dimensional Ising model were given as examples with the promise that more universality classes would be considered when the appropriate models had been introduced. We are now in a position to do this.

Universality classes which correspond to the models we have discussed in this chapter are listed in Table 3.1, together with an explicit description of the symmetry of the order parameter, physical examples and the values of the critical exponents. This is a far from exhaustive

⁴Kogut, J. B. (1979). *Reviews of Modern Physics*, **51**, 659.

⁵Kosterlitz, J. M. and Thouless, D. J. (1978). Two-dimensional physics. In *Progress in Low Temperature Physics*, Vol VIII (ed. D. I. Brewer), p.371. (North-Holland, Amsterdam).

Table 3.1. Universality classes

Universality class	Symmetry of order parameter	α	β	γ	δ	ν	η	Physical examples
2-d Ising	2-component scalar	0 (log)	1/8	7/4	15	1	1/4	some adsorbed mono e.g. H on Fe
3-d Ising	2-component scalar	0.10	0.33	1.24	4.8	0.63	0.04	phase separation, flu order-disorder e.g. β
3-d X-Y	2-dimensional vector	0.01	0.34	1.30	4.8	0.66	0.04	superfluids, supercon
3-d Heisenberg	3-dimensional vector	-0.12	0.36	1.39	4.8	0.71	0.04	isotropic magnets
mean-field		0 (dis.)	1/2	1	3	1/2	0	
2-d Potts, $q=3$ $q=4$	q -component scalar	1/3 2/3	1/9 1/12	13/9 7/6	14 15	5/6 2/3	4/15 1/4	some adsorbed mono e.g. Kr on graphite

3.5

3.6

3.6 Discussion

list, but it includes many of the common experimental systems. There are two questions which it is interesting to ask at this point, although a full explanation will not be forthcoming until later. Firstly, what universality class will a magnet that is neither strictly isotropic nor infinitely anisotropic, that is $J_x \neq J_z \neq 0$ in the Hamiltonian (3.8), belong to? This is the most common situation in reality. It turns out that any anisotropy in the Hamiltonian, however weak, will eventually, as the system moves towards the critical temperature, drive the critical exponents away from Heisenberg values. The crossover temperature is determined by the strength of the anisotropy. If this is weak the critical behaviour will be Heisenberg-like over a wide range of temperatures and Ising or X-Y exponents may only be realized too close to the critical temperature to be experimentally observable. If the interaction J_z in the Hamiltonian (3.8) dominates, the exponents will cross over to Ising values; if J_x is the stronger interaction the asymptotic critical behaviour will be X-Y like. Crossover is discussed further in Section 8.3.1.

A second point to note is that for dimensions $d \geq 4$ the exponents of the Ising, X-Y, and Heisenberg models become the same and take so-called mean-field values. The mean-field theories which are used to calculate these exponents are described in the next chapter. It is somewhat surprising that the exponents should suddenly lock into a dimensionality-independent value. The explanation of this will need the renormalization group. Note that as the dimensionality increases the Potts model (except for $q = 2$) does not show the same behaviour but has a first-order transition.

In this chapter we have introduced several models and given examples of how they can describe experimental systems. We close by summarizing the importance of the approach of using simple models and discussing more generally why and to what extent they can give us full information about real systems whose behaviour is determined by complicated many-body interactions.

The prime advantage of using model systems is that they can be chosen to be tractable theoretically and therefore the details of their behaviour can be understood with some confidence. In particular, the aim is to extract a clear understanding of the physics leading to the behaviour which, it is hoped, will be mirrored in the real compound. Once the basic principles have been established various refinements or perturbations can be included in the models. Examples would be

effects of more complicated interactions, of defects, or of more realistic lattice structures. By ascertaining the robustness of the system to these perturbations it should be possible to establish whether they will significantly change the important physics and hence whether they are essential to model realistically a particular experimental system.

Often it is possible to go further than this and obtain a quantitative fit to experimental data, rather than just a qualitative understanding of it. For example, because critical exponents are universal and depend only on the dimensionality of space and the symmetry of the order parameter, a model has only to incorporate these properly to predict the correct critical behaviour.

It is often also feasible to obtain the behaviour of the thermodynamic functions throughout the whole range of temperature. This is because the interactions relevant to the physics under consideration can be mapped on to a few effective short-range terms. For example, for the case of hydrogen on iron, described in Section 3.1.2, where we are just looking at the ordering of the adsorbate, details of the iron-iron interactions are not important: they can just be considered to define a lattice of adsorption sites for the hydrogen atoms. Moreover, the complicated many-body interactions between the adsorbed atoms themselves can be well approximated by a simple spin Hamiltonian.

Exactly which interactions need to be included and their magnitudes must be confirmed by fitting to experimental results or by returning to a first principles calculation based on model atomic potentials. Hence a calculation of the critical temperature itself is in the realm of the band theorist and quantum chemist.

It is reassuring to be able to observe examples of spin models in nature. They also stand as interesting mathematical problems in their own right. How to study them forms the text of the remainder of this book.

3.7 Problems

3.1 Find the ground state (stable configuration at $T = 0$) of the following spin models:

(i) The one-dimensional Ising model with first and second neighbour interactions

$$\mathcal{H} = -J_1 \sum_i s_i s_{i+1} - J_2 \sum_i s_i s_{i+2}, \quad s_i = \pm 1.$$

Consider both positive and negative values of the exchange parameters.

(ii) The one-dimensional, p -state chiral clock model

$$\mathcal{H} = -J \sum_i \cos\{2\pi(n_i - n_j + \Delta)/p\}, \quad n_i = 1, 2, \dots, p$$

for $J > 0$ and all values of Δ .

(iii) The spin-1 Ising model on a simple cubic lattice

$$\mathcal{H} = -J \sum_{\langle ij \rangle} s_i s_j - K \sum_{\langle ij \rangle} s_i^2 s_j^2 - D \sum_i s_i^2 \quad s_i = \pm 1, 0.$$

Consider both positive and negative values of the exchange interactions.

(iv) The antiferromagnetic spin-1/2 Ising model on a triangular lattice

$$\mathcal{H} = J \sum_{\langle ij \rangle} s_i s_j, \quad s_i = \pm 1$$

with $J > 0$.

3.2 Show that on the square lattice the spin-1 Ising model, described by the Hamiltonian (3.6), has the same symmetry as the three-state Potts model, described by the Hamiltonian (3.7), if

$$D + 2(J + K) = 0, \quad H = 0, \quad L = 0.$$

3.3 The one-dimensional, p -state clock model is described by the Hamiltonian

$$\mathcal{H} = -J \sum_{\langle ij \rangle} \cos\{2\pi(n_i - n_j)/p\}, \quad n_i = 1, 2, \dots, p.$$

Show that this model is equivalent to the q -state Potts model

$$\mathcal{H} = -J \sum_{\langle ij \rangle} \sigma_i \sigma_j, \quad \sigma_i = 1, 2, \dots, q$$

for $p = q = 2$ and $p = q = 3$ but not for higher values of p .

3.4 The Ising lattice gas is described by a Hamiltonian

$$\mathcal{H} = -J_L \sum_{\langle ij \rangle} s_i s_j t_i t_j - K_L \sum_{\langle ij \rangle} t_i t_j - D_L \sum_i t_i$$

$$s_i = \pm 1, \quad t_i = 0, 1.$$

Find a transformation which demonstrates the equivalence of this model to the spin-1 Ising model defined by the Hamiltonian (3.6) with $H = L = 0$.

tricritical point $a = b = 0$. Sketch the form of the free energy in each region of the (a, b) plane, on the transition lines, and at the tricritical point⁵.

4.7 (i) Show that the critical parameters of the Van der Waals equation of state for a fluid (eqn 4.49) are

$$P_c = a/27b^2, \quad V_c = 3b, \quad NkT_c = 8a/27b.$$

(ii) Hence show that, when written in terms of reduced variables

$$p = P/P_c, \quad v = V/V_c, \quad t = T/T_c,$$

the equation takes the universal form

$$(p + 3/v^2)(v - 1/3) = 8t/3.$$

This is the law of corresponding states. Although the quantitative form of the equation is incorrect for fluids in three dimensions near the critical point, the idea of an equation of state which, when written in reduced variables, is universal has been very important in the development of the theory of critical phenomena. See Fig. 2.2 for experimental evidence.

(iii) Obtain values for the critical exponents β , γ , δ of the Van der Waals theory and confirm that they take mean-field values⁶.

⁵For an analysis which includes the terms in odd powers of m see Appendix A of Sarbach, S. and Fisher, M. E. (1979). *Physical Review*, B20, 2797.

⁶To obtain a value for α requires knowledge of the free energy. See Thompson, C. J. (1988). *Classical equilibrium statistical mechanics*, p. 84. (Clarendon Press, Oxford).

5

The transfer matrix

The aim of this chapter is to describe how transfer matrices can be used to solve one-dimensional classical spin models. The idea is to write down the partition function in terms of a matrix, the transfer matrix. The thermodynamic properties of the model are then wholly described by the eigenspectrum of the matrix. In particular the free energy per spin in the thermodynamic limit depends only on the largest eigenvalue and the correlation length only on the two largest eigenvalues through simple formulae.

The simplest application of the transfer matrix technique is to the exact solution of one-dimensional spin models with a finite number of neighbours per site and a finite number of spin states. Transfer matrices have, however, also proved very useful in the solution of exactly solvable two-dimensional models; now the matrices are infinite-dimensional and their analysis requires sophisticated mathematics¹.

5.1 Setting up the transfer matrix

We shall use the one-dimensional Ising model in a magnetic field as an explicit example of how to set up a transfer matrix. This model is described by the Hamiltonian

$$\mathcal{H}_N = -J \sum_{i=0}^{N-1} s_i s_{i+1} - H \sum_{i=0}^{N-1} s_i \quad (5.1)$$

where we shall, for convenience, take periodic boundary conditions, that is identify $s_N \equiv s_0$. The choice of boundary conditions becomes irrelevant in the thermodynamic limit, $N \rightarrow \infty$.

¹Baxter, R. J. (1982). *Exactly solved models in statistical mechanics*. (Academic Press, London and San Diego).

The partition function, written out in some detail, is

$$Z = \sum_{\{s\}} e^{\beta J(s_0 s_1 + s_1 s_2 + \dots + s_{N-1} s_N)} + \beta H(s_0 + s_1 + \dots + s_{N-1}) \quad (5.2)$$

where $\{s\}$ represents the trace over all possible states of the system, that is the sum over $s_i = \pm 1$ for all spins s_i . The important property of eqn (5.2) that allows it to be represented as a product of matrices is that it can be rearranged into products of terms each depending only on nearest neighbour pairs

$$\begin{aligned} Z &= \sum_{\{s\}} e^{\beta J s_0 s_1 + \beta H(s_0 + s_1)/2} e^{\beta J s_1 s_2 + \beta H(s_1 + s_2)/2} \dots \\ &\dots e^{\beta J s_{N-1} s_N + \beta H(s_{N-1} + s_N)/2} \\ &\equiv \sum_{\{s\}} \mathbf{T}_{0,1} \mathbf{T}_{1,2} \dots \mathbf{T}_{N-1,0} \end{aligned} \quad (5.3)$$

where

$$\mathbf{T}_{i,i+1} = e^{\beta s_i s_{i+1} + \beta H(s_i + s_{i+1})/2} \quad (5.5)$$

are the elements of a matrix \mathbf{T} with rows labelled by the values of s_i and columns by the values of s_{i+1} . Writing out \mathbf{T} explicitly for the model we are considering

$$\begin{array}{cc} s_{i+1} = 1 & s_{i+1} = -1 \\ s_i = 1 & \begin{pmatrix} e^{\beta(J+H)} & e^{-\beta J} \\ e^{-\beta J} & e^{\beta(J-H)} \end{pmatrix} \\ s_i = -1 & \end{array} \quad (5.6)$$

Equation (5.4) is easily simplified by noting that it is a matrix product written in terms of the components of the matrix \mathbf{T} . Taking the trace over the spins $i = 1, 2, \dots, N-1$ corresponds to performing the product

$$Z_N = \sum_{s_0=\pm 1} (\mathbf{T}^N)_{0,0} \quad (5.7)$$

so that only the summation over s_0 of the diagonal elements of \mathbf{T}^N remains. This is just the trace of \mathbf{T}^N which is most usefully expressed in terms of the eigenvalues λ_i of \mathbf{T}

$$Z_N = \sum_i \lambda_i^N \quad (5.8)$$

Although we have used the example of the one-dimensional Ising model to enable us to display an explicit formula at each step, eqn (5.8) is a general result.

The transfer matrix method is useful whenever the partition function can be factorized in a form like eqn (5.3) and hence expressed as a product of matrices. A common application is to one-dimensional classical spin systems with finite-range interactions. The size of the transfer matrix depends on the number of spin states per site and on the range of the interactions. For example, for the nearest neighbour q -state Potts model it is $q \times q$. For the one-dimensional Ising model with first and second neighbour interactions the rows and columns are labelled by s_i, s_{i+1} and s_{i+2}, s_{i+3} respectively and hence the matrix is 4×4 . As the model gets more complicated the usefulness of the formalism depends on whether the transfer matrix can be diagonalized analytically or numerically.

A pictorial way of thinking of the transfer matrix is that it builds up the lattice step by step. Multiplying by the R^{th} power of \mathbf{T} adds the spin s_R and traces over the spin s_{R-1} . Hence this step can be considered to add the bond between spins $R-1$ and R . Any further terms in Z cannot depend on the value of s_{R-1} as the trace has already been taken over this spin.

5.2 The free energy

The power of the transfer matrix formalism becomes apparent in the formula for the free energy. We shall now leave the example of the Ising model and consider a general transfer matrix \mathbf{T} of size $n \times n$. If the eigenvalues, listed in terms of decreasing modulus, are labelled $\lambda_0, \lambda_1, \lambda_2 \dots, \lambda_{n-1}$ then, in the thermodynamic limit, the free energy per spin is given by

$$f = -kT \lim_{N \rightarrow \infty} \frac{1}{N} \ln Z_N \quad (5.9)$$

$$= -kT \lim_{N \rightarrow \infty} \frac{1}{N} \ln \left\{ \lambda_0^N \left(1 + \sum_{i=1}^{n-1} \frac{\lambda_i^N}{\lambda_0^N} \right) \right\} \quad (5.10)$$

But, as $N \rightarrow \infty$, $(\lambda_i/\lambda_0)^N \rightarrow 0$ because the ratio is less than 1 and hence

$$f = -kT \ln \lambda_0 \quad (5.11)$$

This is an important result because it is often much easier to calculate λ_0 than the entire spectrum of a matrix.

It is not necessary to worry about degeneracy in λ_0 because transfer matrices can be proved to belong to a class of matrices with non-degenerate, positive largest eigenvalue λ_0 , thus giving a physically

sensible free energy². We have assumed that the λ_i are real. This is not necessarily the case for $i \neq 0$ but the formula (5.11) still holds (see problem 5.3).

5.3 The correlation function

A second important quantity which is simply related to the eigenvalues of the transfer matrix is the correlation length. To calculate this we need the spin-spin correlation function which serves as an example of how to obtain averages of products of spins using transfer matrices. We recall from Chapter 2 the definitions of Γ_R , the two-spin correlation function, and ξ , the correlation length,

$$\Gamma_R = (\langle s_0 s_R \rangle - \langle s_0 \rangle \langle s_R \rangle), \quad (5.12)$$

$$\xi^{-1} = \lim_{R \rightarrow \infty} \left\{ -\frac{1}{R} \ln |\langle s_0 s_R \rangle - \langle s_0 \rangle \langle s_R \rangle| \right\}. \quad (5.13)$$

Consider first the calculation of

$$\langle s_0 s_R \rangle_N = \frac{\sum_{\{s\}} s_0 s_R e^{-\beta \mathcal{H}_N}}{\sum_{\{s\}} e^{-\beta \mathcal{H}_N}} \equiv \frac{1}{Z_N} \sum_{\{s\}} s_0 s_R e^{-\beta \mathcal{H}_N} \quad (5.14)$$

where the subscript N denotes that we are again considering a ring of N spins. Z_N is known from eqn (5.8) and the numerator can be written in a form analogous to eqn (5.4)

$$\begin{aligned} \sum_{\{s\}} s_0 s_R e^{-\beta \mathcal{H}_N} &= \sum_{\{s\}} s_0 \mathbf{T}_{0,1} \mathbf{T}_{1,2} \cdots \mathbf{T}_{R-1,R} s_R \mathbf{T}_{R,R+1} \cdots \mathbf{T}_{N-1,0} \\ &= \sum_{s_0 s_R} s_0 (\mathbf{T}^R)_{0,R} s_R (\mathbf{T}^{N-R})_{R,0}. \end{aligned} \quad (5.15)$$

Let \mathbf{T} have eigenvectors $|\vec{u}_i\rangle$ corresponding to the eigenvalues λ_i , $i = 0, 1, 2, \dots, n-1$. It will also be useful to define the diagonal matrix s_R

²This is the Perron-Frobenius theorem which is discussed in Horn, R. A. and Johnson, C. A. (1985). *Matrix analysis*, p.508. (Cambridge University Press, Cambridge).

with eigenvalues equal to the possible values of s_R and corresponding eigenvectors $\langle \vec{s}_R | = \langle 00 \dots 010 \dots 00 \rangle$. Making use of the formulae

$$s_R = \sum_{\vec{s}_R} |\vec{s}_R\rangle s_R \langle \vec{s}_R|, \quad (5.16)$$

$$\mathbf{T} = \sum_i |\vec{u}_i\rangle \lambda_i \langle \vec{u}_i|, \quad (5.17)$$

and

$$(\mathbf{T}^R)_{0,R} = \sum_i \langle \vec{s}_0 | \vec{u}_i \rangle \lambda_i^R \langle \vec{u}_i | \vec{s}_R \rangle \quad (5.18)$$

eqn (5.15) becomes

$$\sum_{\{s\}} s_0 s_R e^{-\beta \mathcal{H}_N} = \sum_{s_0 s_R} \sum_{i,j} s_0 \langle \vec{s}_0 | \vec{u}_i \rangle \lambda_i^R \langle \vec{u}_i | \vec{s}_R \rangle s_R \langle \vec{s}_R | \vec{u}_j \rangle \lambda_j^{N-R} \langle \vec{u}_j | \vec{s}_0 \rangle. \quad (5.19)$$

Moving the final matrix element to the beginning of the product and using eqn (5.16):

$$\sum_{\{s\}} s_0 s_R e^{-\beta \mathcal{H}_N} = \sum_{i,j} \langle \vec{u}_j | s_0 | \vec{u}_i \rangle \lambda_i^R \langle \vec{u}_i | s_R | \vec{u}_j \rangle \lambda_j^{N-R}. \quad (5.20)$$

Hence, recalling the formula (5.8) for Z ,

$$\langle s_0 s_R \rangle_N = \frac{\sum_{i,j} \langle \vec{u}_j | s_0 | \vec{u}_i \rangle \left(\frac{\lambda_i}{\lambda_0} \right)^R \langle \vec{u}_i | s_R | \vec{u}_j \rangle \left(\frac{\lambda_j}{\lambda_0} \right)^{N-R}}{\sum_k \left(\frac{\lambda_k}{\lambda_0} \right)^N} \quad (5.21)$$

where we have divided through by λ_0 . It is then easy to see that in the thermodynamic limit only the terms in $j = 0$ and $k = 0$ survive

$$\langle s_0 s_R \rangle = \lim_{N \rightarrow \infty} \langle s_0 s_R \rangle_N = \sum_i \left(\frac{\lambda_i}{\lambda_0} \right)^R \langle \vec{u}_0 | s_0 | \vec{u}_i \rangle \langle \vec{u}_i | s_R | \vec{u}_0 \rangle \quad (5.22)$$

$$\begin{aligned} &= \langle \vec{u}_0 | s_0 | \vec{u}_0 \rangle \langle \vec{u}_0 | s_R | \vec{u}_0 \rangle + \sum_{i \neq 0} \left(\frac{\lambda_i}{\lambda_0} \right)^R \langle \vec{u}_0 | s_0 | \vec{u}_i \rangle \langle \vec{u}_i | s_R | \vec{u}_0 \rangle \\ &= \langle s_0 \rangle \langle s_R \rangle + \sum_{i \neq 0} \left(\frac{\lambda_i}{\lambda_0} \right)^R \langle \vec{u}_0 | s_0 | \vec{u}_i \rangle \langle \vec{u}_i | s_R | \vec{u}_0 \rangle \end{aligned} \quad (5.23)$$

where in the final step we have used

$$\langle s_R \rangle = \langle \vec{u}_0 | s_R | \vec{u}_0 \rangle \quad (5.24)$$

which can be proved by a method entirely analogous to that followed above (see problem 5.1).

The correlation function (5.12) then follows immediately as

$$\Gamma_R = \sum_{i \neq 0} \left(\frac{\lambda_i}{\lambda_0} \right)^R \langle \vec{u}_0 | s_0 | \vec{u}_i \rangle \langle \vec{u}_i | s_R | \vec{u}_0 \rangle. \quad (5.25)$$

Note that it depends on all the eigenvalues and eigenvectors of the transfer matrix. A much simpler formula is obtained for the correlation length (5.13). Taking the limit $R \rightarrow \infty$ the term $i = 1$ dominates the sum in eqn (5.25) and hence

$$\begin{aligned} \xi^{-1} &= \lim_{R \rightarrow \infty} \frac{1}{R} \ln \left\{ \left(\frac{\lambda_1}{\lambda_0} \right)^R \langle \vec{u}_0 | s_0 | \vec{u}_1 \rangle \langle \vec{u}_1 | s_R | \vec{u}_0 \rangle \right\} \\ &= -\ln(\lambda_1/\lambda_0). \end{aligned} \quad (5.26)$$

This formula has proved invaluable in work involving large transfer matrices—it is far easier numerically to find a small number of dominant eigenvalues than to completely diagonalize the matrix.

A point worth noting is that usually the Hamiltonian considered is translationally invariant. Hence the product of matrix elements in eqn (5.25) can be rewritten

$$\langle \vec{u}_0 | s_0 | \vec{u}_i \rangle \langle \vec{u}_i | s_R | \vec{u}_0 \rangle = \langle \vec{u}_i | s_0 | \vec{u}_0 \rangle^2. \quad (5.28)$$

We have also ignored the possibility that λ_i , $i \neq 0$, can be complex. This case is followed through in problem 5.3.

5.4 Results for the Ising model

Let us now return to the example considered in Section 5.1, the nearest neighbour Ising model in a magnetic field, to obtain explicit results for the quantities discussed in Sections 5.2 and 5.3. Diagonalizing the matrix (5.6) gives

$$\lambda_{0,1} = e^{\beta J} \cosh \beta H \pm \sqrt{e^{2\beta J} \sinh^2 \beta H + e^{-2\beta J}}, \quad (5.29)$$

$$\langle \vec{u}_0 | = (\alpha_+, \alpha_-), \quad \langle \vec{u}_1 | = (\alpha_-, -\alpha_+) \quad (5.30)$$

where

$$\alpha_{\pm}^2 = \frac{1}{2} \left(1 \pm \frac{e^{\beta J} \sinh \beta H}{\sqrt{e^{2\beta J} \sinh^2 \beta H + e^{-2\beta J}}} \right). \quad (5.31)$$

Using eqns (5.29)–(5.31) we shall write down expressions for the free energy per spin f , the magnetization per spin $\langle s \rangle$, the correlation function Γ , and the correlation length ξ , and check that they behave in a sensible way.

5.4.1 The free energy

From eqns (5.11) and (5.29)

$$f = -kT \ln \left\{ e^{\beta J} \cosh \beta H + \sqrt{e^{2\beta J} \sinh^2 \beta H + e^{-2\beta J}} \right\}. \quad (5.32)$$

As $\beta \rightarrow \infty$

$$f \rightarrow -kT \ln \{ e^{\beta J} (\cosh \beta H + \sinh \beta H) \} = -J - H \quad (5.33)$$

which is the energy per spin as expected.

5.4.2 The magnetization

This can be obtained either by differentiating the negative of the free energy with respect to the magnetic field H , or by using eqn (5.24)

One obtains

$$\langle s \rangle = (\alpha_+, \alpha_-) \begin{pmatrix} 1 & 0 \\ 0 & -1 \end{pmatrix} \begin{pmatrix} \alpha_+ \\ \alpha_- \end{pmatrix} \quad (5.34)$$

$$= \frac{e^{\beta J} \sinh \beta H}{\sqrt{e^{2\beta J} \sinh^2 \beta H + e^{-2\beta J}}}. \quad (5.35)$$

For non-interacting spins $J = 0$ (or equivalently $T = \infty$), this reduces to

$$\langle s \rangle = \tanh \beta H \quad (5.36)$$

as expected for a paramagnet. In zero field at any finite temperature $\langle s \rangle = 0$, as expected from the symmetry of the model, unless one takes the temperature to zero with H finite and then the field to zero

$$\lim_{H \rightarrow 0^+} \lim_{T \rightarrow 0} \langle s \rangle = \pm 1 \quad (5.37)$$

showing that there is a phase transition at zero temperature to a first ordered ground state.

5.4.3 The correlation function

From eqn (5.25)

$$\Gamma_R = \left(\frac{\lambda_1}{\lambda_0} \right)^R \frac{e^{-2\beta J}}{e^{2\beta J} \sinh^2 \beta H + e^{-2\beta J}}. \quad (5.38)$$

For zero field this simplifies to

$$\Gamma_R(H = 0) = \tanh^R \beta J. \quad (5.39)$$

The zero-field correlation function is plotted as a function of H at different temperatures in Fig. 5.1. Note the expected decay with T

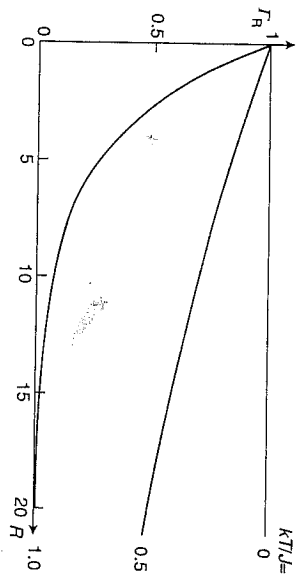


Fig. 5.1. Dependence of the spin-spin correlation function of the one-dimensional Ising model in zero field on distance and temperature.

all $T \neq 0$. If the coupling is antiferromagnetic ($J < 0$) the correlation function changes sign for odd R .

5.4.4 The correlation length

From eqn (5.27)

$$\xi^{-1} = -\ln \left\{ \frac{e^{\beta J} \cosh \beta H - \sqrt{e^{2\beta J} \sinh^2 \beta H + e^{-2\beta J}}}{e^{\beta J} \cosh \beta H + \sqrt{e^{2\beta J} \sinh^2 \beta H + e^{-2\beta J}}} \right\} \quad (5.40)$$

Check that as $T \rightarrow 0$, $\xi^{-1} \rightarrow 0$ signalling the expected phase transition and that as $T \rightarrow \infty$, $\xi^{-1} \rightarrow \infty$.

5.5 Problems

5.1 Prove that, in the thermodynamic limit, the average value of the spin $\langle s \rangle$ is given by

$$\langle s \rangle = \langle \vec{u}_0 | \mathbf{s} | \vec{u}_0 \rangle$$

where \mathbf{s} is the diagonal matrix with eigenvalues equal to the possible values of the spin and $|\vec{u}_0\rangle$ is the eigenvector corresponding to the largest eigenvalue of the transfer matrix.

5.2 (i) Write down the transfer matrix for the one-dimensional, q -state Potts model which is described by the Hamiltonian

$$\mathcal{H} = -J \sum_i \delta_{\sigma_i \sigma_{i+1}}, \quad \sigma_i = 1, 2, \dots, q.$$

(ii) Show that the largest eigenvalue is $e^{\beta J} + q - 1$ and that the remaining eigenvalues are all degenerate and take the value $e^{\beta J} - 1$.

(iii) Write down expressions for the free energy and correlation length of the model and show that they take sensible values in the limits of zero and infinite temperature.

5.3 Write down the transfer matrix for the one-dimensional spin-1 Ising model in zero field which is described by the Hamiltonian

$$\mathcal{H} = -J \sum_i s_i s_{i+1}, \quad s_i = \pm 1, 0.$$

Hence calculate the free energy per spin of this model and show that it has the expected behaviour in the limits $T \rightarrow 0$ and $T \rightarrow \infty$.

[Answer: $f = -kT \ln \{ (1 + 2 \cosh \beta J + [(2 \cosh \beta J - 1)^2 + 8]^{1/2}) / 2 \}$.]

5.4 Consider a transfer matrix with largest eigenvalue λ_0 whose eigenvalues of second largest modulus form a complex conjugate pair $|\lambda_1| e^{\pm i\theta}$. Prove that the correlation length is given by

$$\xi^{-1} = -\ln(|\lambda_1| / \lambda_0)$$

and that the correlations decay with a wavevector θ .

5.5 The one-dimensional, three-state chiral clock model is described by the Hamiltonian

$$\mathcal{H} = -J \sum_i \cos\{2\pi(n_i - n_{i+1} + \Delta)/3\}, \quad n_i = 0, 1, 2.$$

(i) Write down the transfer matrix and show that its eigenvalues and eigenvectors are

$$\lambda_0 = a + b + c \quad |\vec{u}_0\rangle = \frac{1}{\sqrt{3}}(1, 1, 1)$$

$$\lambda_1 = a + \omega b + \omega^2 c \quad |\vec{u}_1\rangle = \frac{1}{\sqrt{3}}(1, \omega, \omega^2)$$

$$\lambda_2 = \lambda_1^* = a + \omega^2 b + \omega c \quad | \vec{u}_2 \rangle = \frac{1}{\sqrt{3}}(1, \omega^2, \omega)$$

where ω is a complex cube root of unity and

$$a = e^{\beta J} \cos\{2\pi\Delta/3\}, \quad b = e^{\beta J} \cos\{2\pi(\Delta-1)/3\}, \\ c = e^{\beta J} \cos\{2\pi(\Delta+1)/3\}.$$

(ii) Hence determine the free energy f , correlation function Γ_R , correlation length ξ , and wavevector associated with the decay of correlations θ .

(iii) Comment on the limit $\Delta \rightarrow 0$.

[Answers: $f = -kT \ln(a+b+c)$;

$$\Gamma_R = \frac{2}{3} \left(\frac{|\lambda_1|}{\lambda_0} \right)^R \cos R\theta;$$

$$\xi^{-1} = \ln\{(a+b+c)/|a+\omega^2 b + \omega c|\};$$

$$\theta = \tan^{-1}\{\sqrt{3}(b-c)/(2a-b-c)\}].$$

5.6 Show that the transfer matrix for the spin-1/2 Ising model with first and second neighbour interactions

$$\mathcal{H} = -J_1 \sum_i s_i s_{i+1} - J_2 \sum_i s_i s_{i+2}, \quad s_i = \pm 1$$

may be written in terms of $x = e^{\beta J_1}$ and $y = e^{\beta J_2}$ as

$$\begin{array}{c} (s_i, s_{i+1}) \\ 1, 1 \\ 1, -1 \\ -1, 1 \\ -1, -1 \end{array} \begin{pmatrix} 1, 1 & 1, -1 & -1, 1 & -1, -1 \\ x^2 y^2 & x^2 & 1 & y^{-2} \\ x^{-2} & x^{-2} y^2 & y^{-2} & 1 \\ 1 & y^{-2} & x^{-2} y^2 & x^{-2} \\ y^{-2} & 1 & x^2 & x^2 y^2 \end{pmatrix} \begin{array}{c} (s_{i+2}, s_{i+3}) \\ 1, 1 \\ -1, 1 \\ x^2 \\ x^2 y^2 \end{array}$$

if two spins are added by each transfer matrix or

$$\begin{array}{c} (s_i, s_{i+1}) \\ 1, 1 \\ 1, -1 \\ -1, 1 \\ -1, -1 \end{array} \begin{pmatrix} 1, 1 & 1, -1 & -1, 1 & -1, -1 \\ xy & xy^{-1} & 0 & 0 \\ 0 & 0 & x^{-1} y & x^{-1} y^{-1} \\ x^{-1} y^{-1} & x^{-1} y & 0 & 0 \\ 0 & xy^{-1} & xy & xy \end{pmatrix} \begin{array}{c} (s_{i+1}, s_{i+2}) \\ 1, 1 \\ -1, 1 \\ -1, -1 \\ 0 \end{array}$$

if a single spin is added at each step.

An analysis of this model, which circumvents diagonalizing the 4×4 transfer matrix is given in Stephenson, J. (1970). *Canadian Journal of Physics*, 48, 1724.

5.7 A simple model of an interface is the solid-on-solid model illustrated in Fig. 5.2. In each column of the lattice, i , the interface lies at a position n_i which is constrained to be single-valued. Thus overhangs and excitations of the bulk are forbidden. A solid-on-solid Hamiltonian which allows description of the binding of the interface to a substrate at $n_i = 0$ is

$$\mathcal{H} = J \sum_i |n_i - n_{i+1}| - K \sum_i \delta_{n_i, 0}; \quad n_i = 0, 1, 2, \dots$$

(i) Write down the transfer matrix of this model in terms of

$$\omega = e^{-J/kT}, \quad \kappa = e^{K/kT}.$$

(ii) By considering an eigenvector of the form

$$(\psi_0, \cos(q+\theta), \cos(2q+\theta), \dots)$$

show that there is a continuous spectrum of eigenvalues

$$(1-\omega)/(1+\omega) \leq \lambda \leq (1+\omega)/(1-\omega).$$

(iii) Show that, for $\kappa > (1-\omega)^{-1}$, there is also a bound state eigenvector of the form

$$(\psi_0, e^{-\mu}, e^{-2\mu}, \dots)$$

which corresponds to an eigenvalue

$$\lambda_0 = \frac{\kappa(1-\omega^2)(\kappa-1)}{\kappa(1-\omega^2)-1}.$$

(iv) Show that, where it exists, λ_0 is the largest eigenvalue. This means that it dominates the thermodynamics and the interface binds to the substrate at $\kappa_c = (1-\omega)^{-1}$. What is the eigenvector corresponding to the largest eigenvalue at this point?

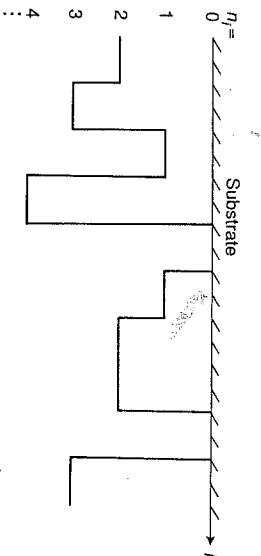


Fig. 5.2. The solid-on-solid model of an interface on a semi-infinite lattice. In each column of the lattice, i , the interface lies at a position $n_i \geq 0$.

6

Series expansions

Exact power series expansions for thermodynamic functions have in the past proved an invaluable aid to understanding the critical behaviour of insoluble models. Indeed, the first suggestions of power law singularities at criticality were based on such analyses. Immediately before the renormalization group was proposed, work using series expansions had led to a large body of evidence that exponents had universal properties, that they were the same above and below the critical temperature, and that mean-field values set in abruptly above four dimensions.

One somewhat intriguing result that has arisen from the [series] analysis of lattices with $d > 3$ is the following: rather than the anticipated mean-field behaviour setting in gradually as $d \rightarrow \infty$ the mean-field critical point exponents appear to be obtained for all values of $d \geq 4$.¹

Series expansions remain, in many cases, one of the most accurate ways of estimating critical exponents. The idea is to find a systematic way of calculating classes of contributions to the partition function which can be obtained exactly and hope that the successive approximations can be extrapolated to give information about critical properties. Two expansion procedures will be considered in this chapter. The first is high temperature series where the Boltzmann factor is expanded in powers of the inverse temperature and the trace taken term by term. In the second, low temperature expansions, configurations are counted in order of their importance as the temperature is increased from zero: starting from the ground state the series is constructed by successively adding terms from 1, 2, 3, ... flipped spins.

As the order of the expansion is increased the number and complexity of contributing terms also increases rapidly. A rule of thumb is

¹Stanley, H. E. (1971). *Introduction to phase transitions and critical phenomena*, Ch. 4. (Oxford University Press, Oxford).

that the work involved in calculating the last term is the same as that needed to calculate all the preceding terms. As we shall see, each term in the series can be represented by graphs on a lattice and constructing the series comes down to counting the allowed graphs, which is usually done using a computer.

The expansions obtained can be used to give an approximation to the thermodynamic properties of a model at low and high temperatures. However, they can be, and more often are, used to study critical properties. The hope is that the expansions are sufficiently well behaved that information about their singularities can be obtained from the limited number of terms available.

The radius of convergence of a series is determined by the singularity which lies nearest to the origin in the complex plane. If this is on the real axis it can, in general, be identified as the critical point whose value and associated exponents can be estimated. Even if the leading singularity lies in the complex plane and is non-physical there are still analysis techniques which can be used to extract the critical behaviour.

There is no rigorous justification that the series expansions are convergent. However, it is widely believed that this procedure works, and not only works but works well—at present the argument is over the third decimal place in series estimates of the exponents of the three-dimensional Ising model. Confidence in the method lies in the large body of circumstantial evidence available. Series expansions agree well with high accuracy Monte Carlo simulations, with renormalization group results, and with exact results for soluble models where these are available. Comparable results are obtained from the analysis of series for different thermodynamic variables and from low and high temperature expansions. Moreover, usually the series behave in a sensible way; as extra terms are added the extrapolated results converge stably. More recently the understanding of the universality of critical exponents has provided another benchmark; the scatter of results for different lattice types provides some estimate of the error bars in the expansion results. However, historically, it was the results from series expansions that suggested universality.

6.1 High temperature series expansions

We first consider the high temperature series expansion for the two-dimensional, zero-field Ising model, defined by the Hamiltonian (3.1) with $H = 0$, on a square lattice. Although this has many simplifying features it illustrates the important ideas involved in the construction

of series expansions. Because, for the Ising model, $s_i s_j = \pm 1$, we may write

$$e^{\beta J s_i s_j} = \cosh \beta J + s_i s_j \sinh \beta J \equiv \cosh \beta J (1 + s_i s_j v). \quad (6.1)$$

$v = \tanh \beta J$ is the natural high temperature expansion variable for this problem: $v \rightarrow 0$ as $T \rightarrow \infty$ as required.

Using eqn (6.1) to rewrite the partition function leads to a form that can be easily expanded in powers of v

$$\mathcal{Z} = \sum_{\{s\}} \prod_{\langle ij \rangle} e^{\beta J s_i s_j} = \sum_{\{s\}} \prod_{\langle ij \rangle} (\cosh \beta J)^B \prod_{\langle ij \rangle} (1 + s_i s_j v) \quad (6.2)$$

$$= (\cosh \beta J)^B \sum_{\{s\}} \prod_{\langle ij \rangle} (1 + s_i s_j v) = (\cosh \beta J)^B \sum_{\{s\}} (1 + v \sum_{\langle ij \rangle} s_i s_j + v^2 \sum_{\langle ij \rangle, \langle kl \rangle} s_i s_j s_k s_l + \dots) \quad (6.4)$$

where B is the number of bonds on the lattice. The aim is to count the number of contributions to \mathcal{Z} which are of order v^n up to as large values of n as possible. The easiest way is to use the correspondence between the terms in eqn (6.4) and graphs on the square lattice. Each product of a pair of spins, $s_i s_j$, can be associated with the bond on the lattice which joins sites i and j . Each term of order v can be represented by a single bond. Terms of order v^2 correspond to two bonds which may or may not, touch and so on. Therefore each term of order v^n is in one-to-one correspondence with a graph with n edges on the square lattice. Examples are shown in Fig. 6.1.

We have to consider not only the number of graphs at a given order but also their contribution to the partition function. Fortunately this is zero in many cases. Because $s_i = \pm 1$

$$\sum_{\{s\}} (s_i^{n_i} s_j^{n_j} s_k^{n_k} \dots) = 2^N \quad (\text{all } n_i \text{ even}) \\ = 0 \quad (\text{otherwise}) \quad (6.5)$$

where N is the number of spins on the lattice. Hence only products which every spin operator appears an even number of times contribute. Graphically these terms correspond to closed loops; no free ends are allowed. Each contributes the same weight, 2^N .

So finding the contribution to the partition function of order n reduced to the problem of counting the number of closed loops of

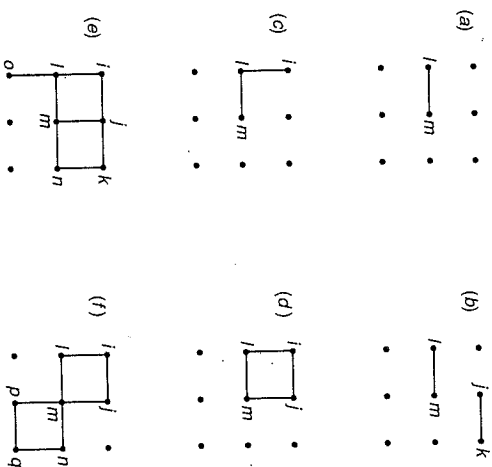


Fig. 6.1. Graphs on the square lattice, each of which corresponds to a product of spins in the sum in eqn (6.4): (a) $s_i s_m$, (b) $s_i s_m s_j s_k$, (c) $s_i s_j^2 s_m$, (d) $s_i^2 s_j^2 s_k^2 s_m^2$, (e) $s_i^2 s_j^2 s_k^2 s_m^2 s_n^2 s_o$, (f) $s_i^2 s_j^2 s_k^2 s_m^2 s_n^2 s_p^2 s_q^2$. Only (d) and (f), where the number of bonds at each vertex is even, give a non-zero contribution to the partition function.

bonds that can be put on the square lattice. Remember that every position and orientation of the loops will give a contribution to the partition function. Terms to order v^{10} are shown in Table 6.1. Reading from the table and using eqn (6.4) gives the leading terms in the high temperature series expansion for the partition function of the two-dimensional Ising model on the square lattice.

$$Z = (\cosh \beta J)^{2N} \{1 + Nv^4 + 2Nv^6 + \frac{1}{2}N(N+9)v^8 + 2N(N+6)v^{10} + O(v^{12})\}. \quad (6.6)$$

The free energy follows as usual from the logarithm of the partition function. Taking the logarithm of eqn (6.6), noting for the square lattice that $B = 2N$, and expanding for small v gives

$$\mathcal{F} = -NkT \left\{ \ln 2 + v^2 + \frac{3}{2}v^4 + \frac{7}{3}v^6 + \frac{19}{5}v^8 + \frac{61}{5}v^{10} + O(v^{12}) \right\}. \quad (6.7)$$

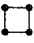





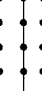






Happily terms with counts proportional to N^2 have dropped out. It can be proved that only terms proportional to N survive at all orders of the expansion, as must be the case if the free energy is to be extensive. This is an example of the linked cluster theorem². It means that it is often possible to formulate rules for calculating the contribution from disconnected diagrams, which are those responsible for terms non-linear in N , without having to obtain the full count.

Having written down an expansion for the free energy the specific heat series can be obtained by differentiation. If a magnetic field is included in the original Hamiltonian—which leads to a relaxation of the constraint on even vertices—the susceptibility series can be generated. This case is considered in problem 6.7. It is also possible to write down series expansions for the correlation functions (see problem 6.6).

How far is it possible to get? The two-dimensional Ising model on a square lattice can be solved exactly in zero field and therefore the series expansion, should one be interested, can be written down to all orders in v . The greatest interest lies in three dimensions where there is continuing progress in refining values for the critical exponents for comparison with increasingly accurate experiments. At the time of writing the susceptibility series for the Ising model on the body-centred cubic lattice is complete to order v^{21} , the specific heat series to order

²Wortis, M. (1974). *Linked cluster expansion*. In *Phase transition and critical phenomena*, Vol 3 (eds C. Domb and M. S. Green), p. 113 (Academic Press, London).

Table 6.1. The configurations, together with their counts, which contribute to the high temperature expansion of the partition function of the Ising model on a square lattice

Order	Contributing graphs	Count
v^4		N
v^6		$2N$
v^8		$N(N-5)/2$
		$4N$
		N
		$2N$
v^{10}		$2N(N-8)$
		$2N$
		$8N$
		$4N$
		$8N$
		$4N$
		$2N$

v^{14} . The argument is about the third decimal place in the values of the critical exponents, the fourth in the value of the critical temperature.

The identity (6.1) which is a property of the spin-1/2 Ising model introduces simplifications helpful to both practitioner and pedagogue. More generally the expansion of the partition function is written

$$Z = \sum_{\{s\}} e^{-\beta\mathcal{H}} = \sum_{\{s\}} (1 - \beta\mathcal{H} + \beta^2\mathcal{H}^2/2! - \dots) \quad (6.8)$$

and the problem is to evaluate the trace of powers of the Hamiltonian. These are just traces of products of spins which it is helpful to identify with graphs on a lattice as before. However, in general, multiple bonds are allowed and the weights depend on the topology of the graphs. Rules pertinent to a given model are drawn up and many ingenious ways of doing the counting which lead to efficient numerical algorithms have been documented in the literature.³

These are details best left to the expert, but it is important to point out that high temperature series have been applied widely to Ising models of all spin magnitudes and with further-neighbour and long-range interactions, other discrete models, such as Potts models, and continuous spin systems. The technique has also proved useful in geometrical problems such as percolation, self-avoiding walks, and in studying the field theories used in particle physics.

6.2 Low temperature series expansions

High temperature expansions cannot give any information about properties below the critical temperature. Therefore, to obtain a complete picture, low temperature expansions are also needed. At low temperatures for models with discrete spin variables⁴ the dominant contribution to the partition function is from states where few spins are flipped relative to their value in the ground state. To exploit this we choose to order the terms in the partition function sum

$$Z = e^{-E_0/kT} \left(1 + \sum_{n=1}^{\infty} \Delta Z_N^{(n)} \right) \quad (6.9)$$

³Domb, C. and Green, M. S. (eds) (1974), *Phase transitions and critical phenomena*, Vol 3. (Academic Press, London).

⁴For Heisenberg models there are no excitations involving discrete energy steps and spin-wave theory is appropriate.

where $\Delta Z_N^{(n)}$ is the sum of Boltzmann factors (with energy, for convenience, being measured relative to the ground state energy E_0) of all states where n spins are flipped relative to the ground state.

For the Ising model each wrong bond associated with flipping a spin has an energy, relative to the ground state, of $2J$ and hence a Boltzmann weight

$$x = e^{-2J/kT}. \quad (6.10)$$

x is the natural expansion variable for the low temperature series. For a single spin flip, which in two dimensions generates four dissatisfied bonds, the Boltzmann weight is x^4 ; for two spin flips it is x^8 unless they are nearest neighbours, in which case only six wrong bonds are generated giving a Boltzmann weight x^6 .

Two factors go to make up the $Z_N^{(n)}$; the number of ways of flipping n spins with given Boltzmann weights, or counts, and the corresponding Boltzmann weights themselves. These are listed in Table 6.2; once the counts are sorted out the Boltzmann weights follow easily. Adding the terms in the table gives the leading behaviour of the low temperature expansion of the partition function of the two-dimensional Ising model:

$$Z = e^{-E_0/kT} \left\{ 1 + Nx^4 + 2Nx^6 + \frac{1}{2}N(N+9)x^8 + 2N(N+6)x^{10} + O(x^{12}) \right\}. \quad (6.11)$$

Note that there is not a one-to-one correspondence between the number of spin flips and the powers of x appearing in the Boltzmann weights. Four-flip terms contribute at orders between x^8 and x^{16} . The expansion is in powers of x , not in the number of spin flips.

6.3 The one-dimensional Ising model

Because the ordering temperature of the one-dimensional Ising model is zero the high temperature series expansion is expected to be convergent at all finite temperatures. It can be written down exactly and easily. For a lattice with free boundaries and N spins there are no closed graphs. Hence, from eqn (6.4),

$$Z = 2^N \cosh^{N-1} \beta J \quad (6.12)$$

where the powers of 2 come from taking the trace of unity and $B = N-1$. For periodic boundary conditions and N spins the graph where all bonds are occupied is allowed and

Table 6.2. The configurations, together with their counts and Boltzmann weights, which contribute to the low temperature expansion of the partition function of the two-dimensional Ising model on a square lattice to order x^{10}

Number of flipped spins	Configuration	Count	Boltzmann weight
1		N	x^4
2		$2N$	x^6
		$N(N-5)/2$	x^8
3		$2N$	x^8
		$4N$	x^8
		$2N(N-8)$	x^{10}
4		$N(N^2 - 15N + 62)/6$	x^{12}
		N	x^8
		$8N$	x^{10}
		$2N$	x^{10}
		$4N$	x^{10}
		$4N$	x^{10}
5		(terms up to x^{16})	x^{10}
		$8N$	x^{10}
6		(terms up to x^{20})	x^{10}
		$2N$	x^{10}
		(terms up to x^{24})	x^{10}

Table 6.3. The configurations, together with their counts and Boltzmann weights, which contribute to the low temperature expansion of the partition function of the one-dimensional Ising model

Number of flipped spins	Configuration	Count	Boltzmann weight
1	•	N	x^4
2	••	N	x^2
3	•••	$N(N-3)/2$	x^4
	••••	N	x^2
	•••••	$N(N-4)$	x^4
	••••••	$N(N^2 - 9N + 20)/6$	x^6
4	•••••••	N	x^2

(terms up to x^8)

$$Z = 2^N \cosh^N \beta J (1 + v^N). \tag{6.13}$$

The first few terms in the low temperature expansion of the one-dimensional Ising model are shown in Table 6.3. Flipping any number of neighbouring spins gives the same Boltzmann weight, x^2 . So the series diverges at $x = 0$ as expected for a model with a zero temperature phase transition.

6.4 Analysis of series expansions

Summing the terms in a series expansion can give an approximation to the low or high temperature behaviour of a given spin model. However, historically there has been far more interest in using the expansions to predict the value of the critical temperature and the associated critical exponents. To do this the singular behaviour must be extracted from a regular expansion.

The radius of convergence of a power series is determined by the

singularity nearest the origin in the complex plane. If this fortuitously lies on the positive real axis it can be identified with the critical temperature and a simple analysis of successive coefficients allows the scaling behaviour to be extracted.

As $T \rightarrow T_c$ a thermodynamic function $Y(t)$ is expected to obey the scaling form

$$Y(t) \sim t^{-\lambda} \tag{6.14}$$

where t is the reduced temperature defined by eqn (2.18). Writing eqn (6.14) in terms of a typical high temperature expansion variable $y = \beta J$ and expanding in y gives

$$\begin{aligned} \tilde{Y}(y) &\sim \left(\frac{y}{y_c}\right)^\lambda \left[1 + \frac{\lambda y}{y_c} + \frac{\lambda(\lambda+1)}{2!} \left(\frac{y}{y_c}\right)^2 + \dots\right. \\ &\quad \left. + \frac{\lambda(\lambda+1) \dots (\lambda+(n-1))}{n!} \left(\frac{y}{y_c}\right)^n + \dots\right] \\ &\equiv \sum_n a_n y^{n+\lambda} \end{aligned} \tag{6.15}$$

where $y_c = \beta_c J$. Comparing the coefficients of $y^{n+\lambda}$ and $y^{n+\lambda+1}$ in the expansion one obtains the simple result

$$\frac{a_n}{a_{n-1}} = \frac{1}{y_c} + \frac{(\lambda-1)}{y_c n}. \tag{6.16}$$

Corrections to scaling will lead to deviations from eqn (6.16) for a finite n . However, the hope is that a plot of a_n/a_{n-1} versus $1/n$ will give an intercept and slope approximating to $1/y_c$ and $(\lambda-1)/y_c$ respectively.

An example is shown in Fig. 6.2 for the reduced susceptibility (that is, the susceptibility divided by its value in the non-interacting limit) series of the spin-1/2 Ising model on lattices of different dimensionalities. These series are well behaved and, even for the low orders shown, converge rather smoothly to the asymptotic behaviour described by eqn (6.16).

Life becomes more complicated if the closest singularity to the origin does not lie on the real axis. The signal of this is that the ratio of successive coefficients does not converge smoothly. In this case a common approach is to calculate the series for the logarithmic derivative of a thermodynamic function

$$\frac{d}{dT} \{\ln Y(t)\} \sim -\frac{\lambda}{T-T_c}. \tag{6.17}$$

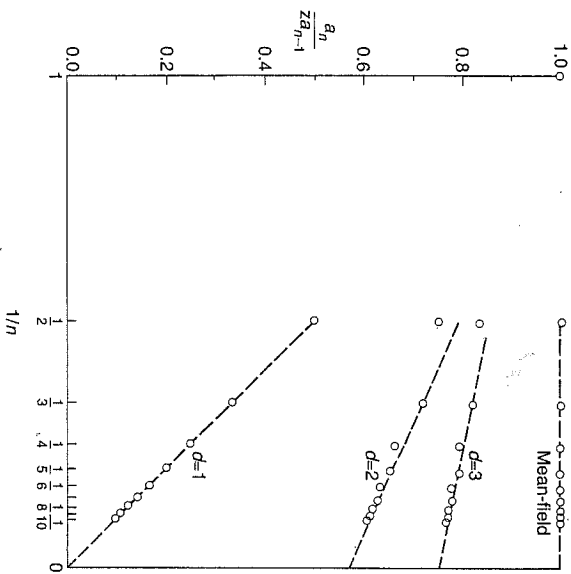


Fig. 6.2. The ratio of successive coefficients, a_n/za_{n-1} , of the reduced susceptibility series of the spin-1/2 Ising model on lattices of different dimensionality plotted against $1/n$. For ease of display the data are normalised by the coordination number of the lattice z . The expected limiting behaviour, given by eqn (6.16), is shown by the dotted lines with the parameters in the equation taken from the exact or best series results available. After Stanley, H. E. (1971). *Introduction to phase transitions and critical phenomena*. (By permission of Oxford University Press, Oxford).

Table 6.4. Estimates of the critical point v_c and the critical exponent γ (in brackets) for the Ising model on a square lattice from the poles and residues of the $[L, M]$ Padé approximants to the series for the logarithmic derivative of the susceptibility. After Gaunt, D. S. and Guttmann, A. J. (1974). *Asymptotic analysis of coefficients*. In *Phase transitions and critical phenomena*, Vol 3 (eds C. Domb and M. S. Green), p.181. (Academic Press, London)

M	$L = M - 1$	$L = M$
1	0.50000	(-2.0000) 0.28571 (-0.6531)
2	0.38871	(-1.4017) 0.41119 (-1.6546)
3	0.40888	(-1.6186) 0.40927 (-1.6257)
4	0.40877 ^a	(-1.6171) 0.41645 (-1.7974)
5	0.41019	(-1.6383) 0.41217 ^a (-1.6823)
6	0.41484	(-1.7782) 0.41413 (-1.7458)
7	0.414249	(-1.7515) 0.414211 (-1.7496)
8	0.414214	(-1.7498) 0.414213 (-1.7498)
9	0.414213	(-1.7498) 0.414214 ^a (-1.7498)
10	0.414202	(-1.7484) 0.414213 (-1.7497)
	exact values	$\sqrt{2} - 1$ $-7/4$

^a approximant with an intervening spurious pole

which has a simple pole at $T = T_c$ with residue $-\lambda$. An $[L, M]$ Padé approximant

$$\frac{P_L(y)}{Q_M(y)} = \frac{p_0 + p_1 y + p_2 y^2 + \dots + p_L y^L}{1 + q_1 y + q_2 y^2 + \dots + q_M y^M} \quad (6.18)$$

is then constructed with the $L + M + 1$ coefficients, p_i, q_i , chosen so that the expansion of the Padé agrees with the first $(L + M + 1)$ terms in the series expansion. The hope is that the denominator of the Padé will reproduce the pole at T_c .

For a series with $n_0 + 1$ terms Padé approximants can be written down for all L, M such that $L + M \leq n_0$. $L \approx M$ usually gives the best results. A comparison of the values which result from different approximants is used to give some feel for the stability of the procedure⁵. An example is given in Table 6.4.

6.5 Problems

6.1 Consider an interface in a one-dimensional Ising model,

$$s_i = -1, \quad i < 0; \quad s_i = 1, \quad i \geq 0.$$

By writing down the energy and entropy associated with such an excitation argue that the one-dimensional Ising model cannot sustain long-range order for any non-zero temperature.

6.2 Show that there is a one-to-one correspondence between the terms in the high and low temperature expansions of the spin-1/2, zero-field Ising model on the square lattice. This model is said to be self-dual.

Hence argue that, if the critical temperature, T_c , is unique, it must be given by

$$e^{-2J/kT_c} = \tanh J/kT_c$$

or

$$J/kT_c = \frac{1}{2} \ln(1 + \sqrt{2}).$$

⁵Relatively little is known about the way in which Padé approximants converge, but see the reference given in Table 6.4 for a summary of the results available.

6.3 The exact result for the spontaneous magnetization per spin in the spin-1/2 Ising model on the square lattice is

$$\langle s \rangle = (1+u)^{1/4} (1-u)^{-1/2} (1-6u+u^2)^{1/8}, \quad u = e^{-4J/kT}. \quad (6.1)$$

Expanding this result gives

$$\langle s \rangle = 1 - 2u^2 - 8u^3 - 34u^4 - 152u^5 - 714u^6 - 3472u^7 - \dots \quad (6.2)$$

(i) Generalize the low temperature expansion for this model given in Section 6.2, to include a non-zero field, H . Hence obtain the series for the zero-field magnetization to terms $O(u^5)$. Check that your answer agrees with the exact result.

(ii) Use the ratio method to obtain an estimate for the critical temperature and the exponent β from the expansion (6.2). Compare with the exact results, $u_c = 3 - 2\sqrt{2}$, $\beta = 1/8$, which follow immediately from eqn (6.19).

6.4 For the three-dimensional spin-1/2 Ising model on a cubic lattice the low temperature expansion for the partition function is

$$Z_N = e^{-\beta N E_0} \{1 + N x^6 + 3N x^{10} + \frac{1}{2} N(N-7)x^{12} + 15N x^{14} + 3N(N-11)x^{16} + O(x^{18})\}$$

where N is the number of spins on the lattice and E_0 is the ground state energy per spin. List the graphs, and the associated counts and Boltzmann weights, that contribute to this expression. Comment on the order of the correction term.

6.5 In performing the low temperature expansion for the q -state Potts model

$$\mathcal{H} = -J \sum_{\langle ij \rangle} \sigma_i \sigma_j, \quad \sigma_i = 1, 2, \dots, q$$

account must be taken of configurations in which the spin f to each of the $(q-1)$ other states. Bearing this in mind list Boltzmann weights that would be associated with the configurations listed in Table 6.2 for the q -state Potts model.

6.6 Use a high temperature series expansion to show that the spin correlation function of the one-dimensional Ising model in zero field is

$$\Gamma_R = \tanh^R \beta J.$$

6.7 This problem deals with the extension of the high temperature series expansion of the spin-1/2 Ising model, developed in Section 6.1, to include a field term.

(i) Show that the partition function of the spin-1/2 Ising model in a field can be written

$$\mathcal{Z} = \cosh^B \beta J \cosh^N \beta H \sum_{\{s\}} \prod_{\langle ij \rangle} (1 + s_i s_j v) \prod_i (1 + s_i y)$$

where $v = \tanh \beta J$; $y = \tanh \beta H$, and B and N are the number of bonds and sites on the lattice respectively.

(ii) Show that the terms in \mathcal{Z} can be represented by graphs on a lattice where each graph with l bonds and m odd vertices contributes a factor $2^N v^l y^m$, and hence that \mathcal{Z} can be rewritten

$$\mathcal{Z} = \cosh^B \beta J (2 \cosh \beta H)^N (1 + S_0 + y^2 S_2 + y^4 S_4 + \dots) \quad (6.21)$$

where $S_m(v, N)$ is the contribution from all graphs with m odd vertices.

Taking the logarithm of eqn (6.21) and using the Linked Cluster Theorem⁶ gives

$$-\beta \mathcal{F} = B \ln \cosh \beta J + N \ln 2 \cosh \beta H + (S'_0 + y^2 S'_2 + y^4 S'_4 + \dots) \quad (6.22)$$

where the prime denotes that, for a given graph, only the part of the count proportional to N must be included.

(iii) Differentiate eqn (6.22) to show that the zero-field susceptibility is

$$\chi = \beta N + 2\beta S'_2.$$

(iv) List the low order graphs with two odd vertices to show that the first few terms in the high temperature expansion of the zero-field susceptibility of the spin-1/2 Ising model on the square lattice are

$$\chi = \beta N + 2\beta(2v + 6v^2 + 18v^3 + \dots).$$

⁶See eqn (6.7) for an explicit example of how this works.

Monte Carlo simulations

It could be argued that current physics research can be divided into three areas—theoretical, experimental, and computational. Numerical approaches, in which systems are mimicked as accurately as possible using a computer or in which computer models are set up to provide well-behaved experimental systems are increasingly providing a bridge between theory and experiment. The limitations on what can be done are set by the computational resources available.

A powerful numerical approach is the Monte Carlo method. It was introduced in 1953 at the dawn of the computer age and its range of applicability and accuracy have continued to increase with the development of more advanced computer technology. One of the simplest and most natural applications, which we shall focus on here, is to discrete spin models. However the technique is very widely used: to study continuous spin systems, fluids, polymers, disordered materials, and lattice gauge theories. Some examples are given at the end of this chapter.

7.1 Importance sampling

A common aim in statistical mechanics is to find the value of a thermodynamic variable, such as the energy or the magnetization, which is a weighted sum over all states in phase space

$$\langle A \rangle = \frac{\sum_{\{s\}} A e^{-\beta \mathcal{H}}}{\sum_{\{s\}} e^{-\beta \mathcal{H}}}.$$

For an Ising model on a lattice of N sites the sum is over 2^N configurations. This is a number which increases very quickly with N and direct evaluation is feasible only for $N \lesssim 40$.

The first way one might try to get round this is to choose randomly a sample of the spin configurations, $\{s\}$, and, weighing them appropriately according to eqn (7.1), work out an estimate of the required average. This approach may be familiar as it is a standard technique used for the evaluation of integrals. However, it fails here because of the rapid variation of the Boltzmann factor, $e^{-\beta E}$, with energy. Very few of the chosen configurations will be weighted by a sufficiently large factor to make a significant contribution to the average and a very unreliable estimate will result.

This problem occurs because only an extremely restricted part of configuration space is important in determining the averages. This we already know from statistical mechanics—the system spends the vast majority of its time in states with thermodynamic parameters within $O(1/\sqrt{N})$ of those describing thermodynamic equilibrium. Therefore it would seem sensible to restrict the sampling to these states. This is a technique known as importance sampling. But how to generate such a set of states? To try to find the probability distribution exactly the partition function would need to be calculated and this is tantamount to going back to the original problem of summing over an impossibly large number of states.

Luckily it turns out to be possible to generate a Markov chain of configurations (a sequence of states each of which depends only on the preceding one) which has the property that \hat{A}_n , the average of A over n , successive states, converges to the thermodynamic average defined in eqn (7.1)

$$\hat{A}_n = \langle A \rangle + O(n^{-1/2}). \tag{7.2}$$

In the limit $n \rightarrow \infty$ each state is weighted by its Boltzmann factor, $e^{-\beta E}$. The disadvantage of this approach is that successive states of the Markov chain are highly correlated, which means that a much longer sequence of sample configurations is needed to achieve a given accuracy than if this were not the case.

The conditions on the transition probability between Markov states needed to achieve the result (7.2) are physically transparent. The transition probability must be normalized. It must be ergodic, that is all states must eventually be accessible. Finally, a sufficient condition is that it must obey detailed balance¹.

This does not specify the transition probability uniquely. The choice often used in Monte Carlo simulations is the Metropolis algorithm. A final state, $\{s\}_f$, is chosen from an initial state, $\{s\}_i$, by

¹Parisi, G. (1988). *Statistical field theory*, p.346. (Addison-Wesley, Wokingham).

flipping one or more spins. The probability that the system is allowed to move from i to f is

$$P(\{s\}_i \rightarrow \{s\}_f) = \begin{cases} e^{-\beta(E_f - E_i)} & \text{if } E_f > E_i \\ 1 & \text{if } E_i \leq E_f \end{cases} \tag{7.3}$$

where E_i and E_f are the energies of the initial and final states respectively.

There is a physically intuitive argument that shows that with this choice of transition probabilities the system tends asymptotically ($n \rightarrow \infty$) to a steady state in which the probability of a given configuration is $e^{-\beta E\{s\}}$. Consider m_r systems in a state $\{s\}_r$ and m_i in a state $\{s\}_i$ such that $E_i < E_r$. Using random numbers it is possible to construct a move such that the *a priori* probability of moving from state r to i is the same as that to move from i to r . (This is feasible but not always the case in realistic simulations.) Then, using eqns (7.3), the number of transitions from r to i and from i to r are

$$M_{r \rightarrow i} \propto m_r \tag{7.4}$$

$$M_{i \rightarrow r} \propto m_i e^{-\beta(E_r - E_i)} \tag{7.5}$$

respectively. The net number of transitions is

$$\Delta M_{r \rightarrow i} \propto \{m_r - m_i e^{-\beta(E_r - E_i)}\}. \tag{7.6}$$

The system will converge to a steady state where $\Delta M_{r \rightarrow i} = 0$ or

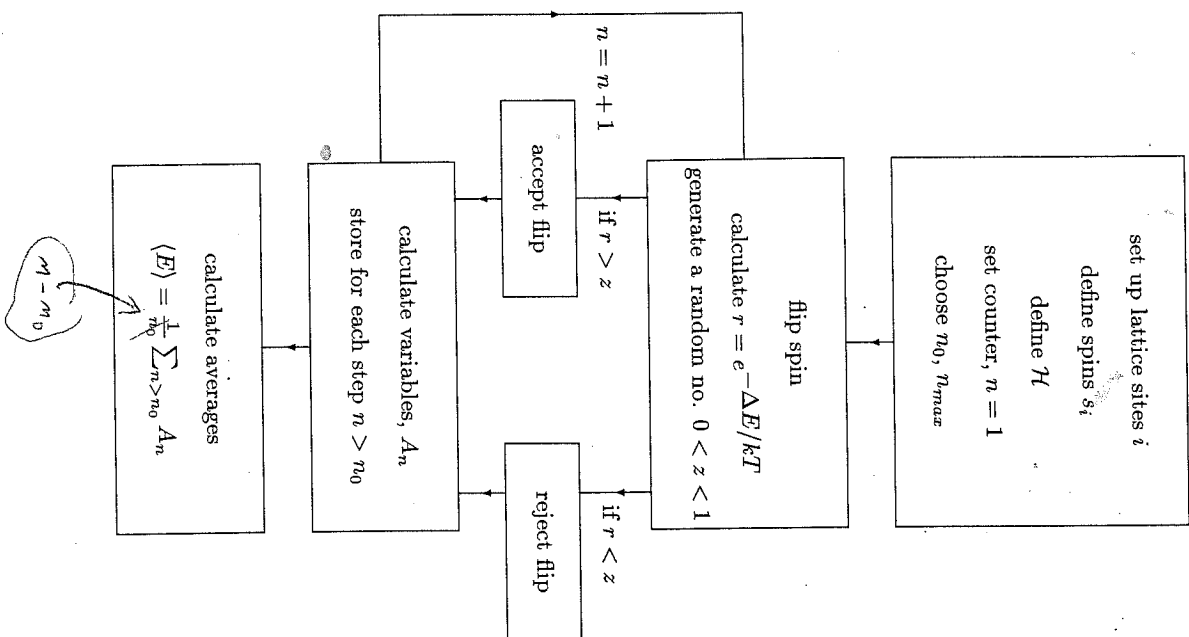
$$\frac{m_r}{m_i} = \frac{e^{-\beta E_r}}{e^{-\beta E_i}}. \tag{7.7}$$

7.2 Practical details

The steps involved in setting up a Monte Carlo simulation for a simple spin model are listed in the flow chart in Table 7.1. This is the basis of the program used to generate the spin configurations in Fig. 1.8. The procedure can be thought of in three parts. We concentrate in this section on the details of how to set up the program and return in the next to a fuller discussion of the problems inherent in the data analysis.

Setting up. The first task is to define a lattice of N sites, i , each of which is occupied by a spin, s_i . This needs to be done in such

Table 7.1. Flow diagram showing the steps in a Monte Carlo calculation of thermodynamic averages for a simple spin model. The system takes n_0 steps to reach equilibrium and the total number of steps is n_{max} .



a way that a record is kept of the neighbours of each spin as its energy will be needed later. The parameters in the problem, such as the temperature and exchange interactions, should also be defined here.

Because N is necessarily finite thought must be given as to what to do with the spins on the boundaries of the system. These can either be left with fewer bonds than usual (free boundary conditions) or assumed to interact with the corresponding spin on the opposite face of the lattice (periodic boundary conditions). The latter option often gives the best results, but care must be taken that the system is not subject to false constraints. For example, simulations on a simple antiferromagnet with periodic boundary conditions can be expected to give inaccurate or spurious results if the length of the lattice is an odd number of spins.

Another consideration is the choice of initial values for the spins. Usually any choice will eventually lead to thermal equilibrium but it is helpful if this happens sooner rather than later. For a simple ferromagnet a ferromagnetically ordered state is likely to provide the most efficient initial configuration at low temperatures; at higher temperatures a random state provides the best starting point. We return to the problems of convergence to equilibrium and finite system size in Sections 7.3.1 and 7.3.3 respectively.

Generating the Markov chain. This is the heart of the program.

It is summarized in the centre portion of Table 7.1. The steps are listed below

1. Select a spin, either randomly or sequentially. Calculate $r = e^{-\Delta E/kT}$ where $\Delta E = E_f - E_i$ is the change in energy associated with a possible spin flip (to a randomly chosen final state if the spin has more than two states).
2. Compare r to a random number $0 < z < 1$.
3. Flip the spin² if $r > z$.
4. Use the final configuration (whether the test spin was flipped or not) to generate the value of any thermodynamic quantity to be averaged. Store this value.

²It is not hard to convince oneself that this procedure reproduces the transition probability given by eqn (7.3): for $\Delta E < 0$, $r > 1$ and hence the spin is always flipped; for $\Delta E > 0$, the probability that $z < r$ is r and hence the spin is flipped with probability $r = e^{-\Delta E/kT}$.

It is important to be aware that any bias in the random number generator will introduce systematic errors into the results. The evidence is that the random number generators built into modern computers have sufficiently good statistics that the errors are insignificant compared to statistical errors. The question of how many configurations are needed to give satisfactory averages is discussed in Section 7.3.2.

Calculating the averages. Average the thermodynamic variables generated at each step of the Markov chain. Care must be taken not to include the initial states where the starting configuration still has an influence. The magnetization and energy are the easiest quantities to calculate as they are just sums over spins or products of spins.

7.3 Considerations in the data analysis

7.3.1 Influence of the starting configuration

During the first iterations of the Monte Carlo procedure the system is not in equilibrium, and hence these configurations cannot be included in the final averages. It can be hard to decide how many steps to exclude. One possibility is to perform several Monte Carlo runs with the same parameters but using different starting configurations. If the results agree to within statistical error it can be concluded that the influence of the starting configuration has been eliminated. A circumstance that can nullify this procedure, which has caused confusion in the past, is that a system can become stuck in a metastable state and feign true thermal equilibrium.

If the simulation is performed near the critical temperature, the additional problem of critical slowing down is encountered. Because of the increasing range of the correlations as criticality is approached, the time for relaxation to equilibrium τ diverges

$$\tau \sim \xi^z \quad (7.8)$$

with $z \sim 2$ for most models. In a finite system the divergence is suppressed; the smaller the system the quicker equilibrium can be achieved for a given temperature. However, at the same time finite-size corrections become more severe and a balance between these and equilibrium times must be struck in the design of a Monte Carlo simulation.

An example of raw data from a Monte Carlo simulation showing the approach to equilibrium and the importance of excluding the initial

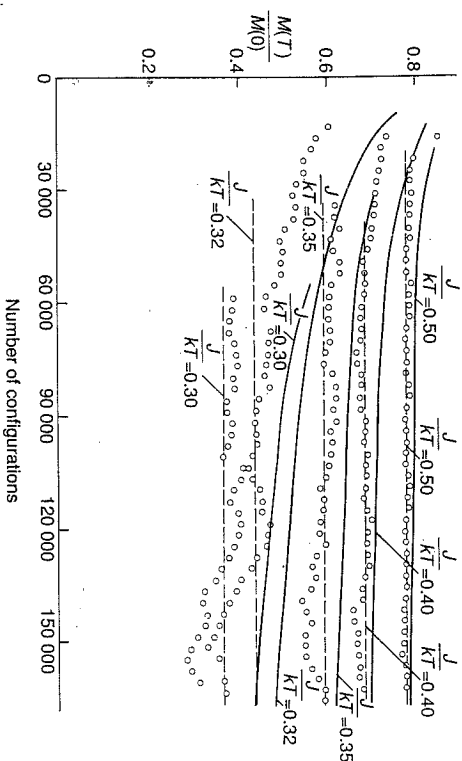


Fig. 7.1. Magnetization of an Ising ferromagnet on a cubic lattice of size $10 \times 10 \times 10$ with periodic boundary conditions plotted as a function of the number of Monte Carlo configurations for different temperatures. Open circles denote averages taken over the three preceding Monte Carlo steps per spin. Full curves give a running average if no initial configurations are excluded. The dashed lines are the final estimates of the magnetization where initial configurations have been excluded. After Binder, K. and Rauch, Z. (1969). *Zeitschrift für Physik*, **219**, 201.

configurations is shown in Fig. 7.1. Note that equilibrium is attained after a few Monte Carlo steps per spin for temperatures sufficiently far from the critical point but a slower relaxation and larger fluctuations are observed closer to T_c ($J/kT_c = 0.22$).

7.3.2 Statistical errors

To obtain reliable results for the equilibrium value of an observable, $\langle A \rangle$, the average must be taken over a time much longer than that over which the Monte Carlo states are correlated. This becomes more difficult near the critical point or if there are metastable states in the system. It can be shown that the deviation of \hat{A}_n from $\langle A \rangle$ is normally distributed in the limit $n \rightarrow \infty$. Thus standard data analysis can be applied to determine the statistical error.

Dividing the equilibrium configurations into independent blocks

and calculating \hat{A} for each block gives a set of essentially independent estimates of $\langle A \rangle$, the variance of which gives a value for the sampling error. The problem is to know when a block of states is long enough that different blocks can indeed be considered mutually independent. A test for this is to perform the analysis using several different block sizes. The blocks are long enough when the variance becomes independent of the block size.

An alternative is to average over several different runs. The disadvantage of this procedure is that the system must be equilibrated afresh for each set of data.

7.3.3 Finite-size corrections

Because it is impossible to simulate an infinite system—for a three-dimensional Ising model $N = (128)^3$ is a realistic size on modern supercomputers—finite-size effects must be taken into account. Away from the critical point, where the correlation length is small compared to the system size, this is usually not a major problem and the parameters of the simulation can be chosen so that the errors due to the limitations in the number of spins are small compared to statistical errors.

The problem becomes much more acute as a continuous phase transition is approached, because on a finite lattice the correlation length is prevented from becoming infinite. As a result any singularities associated with the phase transition are shifted and rounded. The best compromise is to obtain high quality data for lattices of different linear dimension L , and extrapolate to $L = \infty$.

7.4 Examples

7.4.1 The three-dimensional Ising model

A lot of effort has been put into Monte Carlo simulations for the three-dimensional Ising model. This is partly because of its suitability for fast algorithms and partly because of the intrinsic interest in obtaining precise values for the critical parameters. Special purpose machines, in which the time-consuming spin updating is carried out by a specially constructed processor, have been built in several places. These are orders of magnitude cheaper than supercomputers but can only carry out the specific task for which they were designed. They can achieve an accuracy comparable to that obtained by careful programming on the most powerful conventional computers.

As an example of the run times that can be achieved we give some

figures from a machine at Santa Barbara, USA³. This can update 1 spins each second. Lattice sizes of up to $N = 64 \times 64 \times 64$ were used and data for 10^7 – 10^8 Monte Carlo steps per spin collected for each size. At the critical temperature on the largest lattices the time to come to equilibrium was of the order of 7000 Monte Carlo steps per spin.

Using these data the result for the critical temperature was $K_c = J/kT_c = 0.221650(5)$ where the figure in brackets is the estimate of the error in the last digit. This agrees with, and is comparable in accuracy to, the best estimate from series expansions, $K_c = 0.221655(5)^4$. The value obtained for the exponent ratio $\gamma/\nu = 1.98(2)$ is considerably less precise because of the problems of finite-size effects. Better results can be obtained using the Monte Carlo renormalization group, a technique which combines the strengths of the renormalization group and Monte Carlo simulations. This will be described in Chapter 9.

7.4.2 More complicated systems

Although Monte Carlo is particularly well suited to simulations of Ising and other discrete spin models it was originally introduced in relation to fluids and has proved useful both here and in many other contexts. The most fundamental difference between simulations of different systems is in the choice of test configuration.

For example, for fluids, one possibility is to choose a molecule random and allow it to move through a distance chosen at random between 0 and Δ in a random direction. The most accurate results are obtained if Δ is chosen so that approximately half the trials are accepted. Many different models have been considered in the literature ranging from a gas of hard sphere molecules to attempts to incorporate realistic interatomic potentials. Common aims are to calculate equation of state or the pair correlation function.

With today's computational power it is feasible to obtain realistic results for even more complicated systems. One example is solution of polymers, long chain molecules, where Monte Carlo has been particularly useful in looking at properties which depend on the polymer topology rather than the details of the chemistry. Here the so-called reptation technique is one of the most efficient ways of generating suitable sequences of states. Starting from an arbitrary configuration end of one of the chains is removed at random and added to the other

³Barber, M. N., Pearson, R. B., Toussaint, D., and Richardson L. (1985). *Physical Review*, **B32**, 1720.

⁴Adler, J. (1983). *Journal of Physics A: Mathematical and General* **16**, 3585.

end of the chain. As long as the self-avoidance of the chains is preserved the move is accepted according to the usual Metropolis criterion. Results have been obtained for such diverse problems as the changes in chain morphology as the temperature or solvent composition are varied, for the properties of chain molecules at surfaces, and for the dynamics of tangled polymers.

7.5 Problem

7.1 Write a Monte Carlo program to determine the temperature dependence of the energy and magnetization of a two-dimensional Ising model on a square lattice. Choose a lattice size appropriate to the power of the computer you are using. Useful illustrative results can be obtained using lattices of size as small as 6×6 .

Discuss

- (i) the initial conditions used
- (ii) the boundary conditions
- (iii) the number of steps required to achieve thermodynamic equilibrium
- (iv) error bars for the results at each temperature
- (v) the effect of the finite system size.

The renormalization group

The approaches described so far in this book have given a broad phenomenological understanding of critical phenomena. However, although a substantial framework of results and connections has been built up, we have, as yet, no explanations for the following:

1. Continuous phase transitions fall into universality classes characterized by a given value of the critical exponents.
2. For a given universality class there is an upper critical dimension above which exponents take on mean-field values.
3. Relations between exponents, which follow as inequalities from thermodynamics, hold as equalities.
4. Critical exponents take the same value as the transition temperature is approached from above or below.
5. Two-dimensional critical exponents often appear to be rational fractions.

What is needed is a theory, based on the physics of what is happening at the critical point. We argued in Chapter 1 that the special feature of criticality is that the correlation length is infinite and that the critical system is invariant on all length scales. The aim is to write down a (hopefully short, elegant, and comprehensible) mathematical theory which embodies this physics and explains all the observations listed above. A useful theory will also allow the calculation of critical exponents and transition temperatures, if not exactly, then within a accurate and well-controlled approximation scheme.

